UNIVERSITÄT HAMBURG

UNIVERSITÀ DEGLI STUDI DELL'AQUILA

UNIVERSITAT AUTÒNOMA DE BARCELONA

Erasmus Mundus Consortium MathMods

Joint Degree of Master of Science in
Mathematical Modelling in Engineering: Theory, Numerics, Applications

In the framework of the
Consortium Agreement and Award of a Joint/Multiple Degree 2013-2019

Master's thesis

A Study of Non-Local Hughes' Model for Pedestrian Flow

Supervisor

Prof. Debora Amadori

Candidate

Havva Yoldas
Matricola: 228481

2014/2015

Laurea Magistrale in Ingegneria Matematica
Dipartimento di Ingegneria e Scienze dell'Informazione e Matematica
Università degli Studi dell'Aquila

Declaration of Authorship

I, Havva YOLDAŞ, declare that this thesis titled, "A Study of Non-Local Hughes' Model for Pedestrian Dynamics" and the work presented in it are my own. I confirm that:

- This work was done wholly or mainly while in candidature for a research degree at this University.
- Where any part of this thesis has previously been submitted for a degree or any other qualification at this University or any other institution, this has been clearly stated.
- Where I have consulted the published work of others, this is always clearly attributed.
- Where I have quoted from the work of others, the source is always given. With the exception of such quotations, this thesis is entirely my own work.
- I have acknowledged all main sources of help.
- Where the thesis is based on work done by myself jointly with others, I have made clear exactly what was done by others and what I have contributed myself.

Signed: _____

Date: _____

UNIVERSITÀ DEGLI STUDI DELL'AQUILA

Abstract

Faculty of Science
Department of Information Engineering,
Computer Science and Mathematics

Master of Science

A Study of Non-Local Hughes' Model for Pedestrian Dynamics

by Havva YOLDAŞ

We consider the Hughes' model for pedestrian in one dimension and a non-local variant of it. Non-local effects of macroscopic models for traffic flow often interpreted as the deviation of the crowd from the desired direction. This deviation is determined by the average density perceived by the vehicles or pedestrians and it is modeled by a convolution operator acting on the velocity term. We perform simulations of both local and non-local Hughes' model for pedestrian flow by considering two different types of convolution kernels.

Acknowledgements

Öncelikle bana en başından beri güvendikleri ve bu süreçte maddi manevi her türlü desteği sağladıkları için annem Ayşe Yoldaş'a, babam Hayati Yoldaş'a, biricik kardeşlerim Büşra ve Tuğba'ya çok teşekkür ederim.

İlk öğretmenim Filiz Sarıbaş'a ve tüm eğitim hayatım boyunca üzerimde emeği olan bütün öğretmenlerime teşekkür ederim.

I would like to thank my thesis advisor Prof. Debora Amadori, for her guidance, patience and advice. For giving me the freedom to follow my ideas, for her continuous support and help both not only as a teacher but also as a friend.

To Prof. Paola Goatin; it was her guidence and support that I could learn more about traffic flow modeling. To the ACUMES team at INRIA Sophia Antipolis for giving me a chance to work in an intellectual and friendly environment.

To my professors: Pierangelo Marcati, Corrado Lattanzio, Pasquale Palumbo, Leonardo Guidoni and Bruno Rubino for their wonderful lessons during the last two years of MathMods.

To my friends in Mathmods, my classmates and Sandeep for their help, support and friendship. Without them the social and academic life would never have been so interesting and enjoyable.

Contents

List of Figures

List of Tables

Chapter 1

Introduction

1.1 Mathematical models for collective behaviour

Mathematical modeling and simulation of traffic flow for both vehicular and pedestrian dynamics has become a frequent topic of research. Modeling of such complex phenomena brings along analytic, modeling and simulation level challenges. In this section we introduce some approaches which are used to model collective behavior of cars and pedestrians. For other mathematical models and more detailed studies on properties of these models we refer to [3, 9].

1.2 Microscopic models

The main assumption for microscopic models is that every single person or car is trackable individually. The possible trajectories which every agent takes is foreseen. Microscopic models can be differential, if they are based on ordinary differential equations, or nondifferential, otherwise. Since the main work of the thesis deals with a macroscopic model for pedestrian flow, we will not go into details of microscopic models.

1.3 Macroscopic models

The main assumption for macroscopic models for traffic flow is that the number of pedestrians or vehicles is large enough to be interpreted by locally averaged quantities, such as the density ρ and the velocity v, which are time and space dependent variables. The main compound in macroscopic models is the desired vector field $v : \Omega \to \mathbb{R}^2$, where Ω is the domain agents are free to move in. The desired velocity compound is introduced

to model the presence of a target, e.g. exit points, that people want to reach, in the case of pedestrian flow. The desired velocity v is time-independent and is given initially.

1.3.1 First order macroscopic models

First order models consist of one conservation law of the form

$$\frac{\partial \rho}{\partial t} + \frac{\partial \rho}{\partial x}(f(\rho)) = 0, \quad t > 0, \quad x \in \Omega, \tag{1.1}$$

where ρ represents the density and $f(\rho) := \rho v(\rho)$, is the flux which is given in terms of density in order to close the model. $v(\rho)$ is the velocity field.
The equation (1.1) is completed by an initial condition such that $\rho(0, x) = \rho_0(x)$. If the domain Ω is bounded then there will be some boundary conditions on $\partial\Omega$ for any $t > 0$. (1.1) is the mass conservation equation for pedestrians or vehicles which follow the nonlinear velocity field $v(\rho)$ and it is conserved in time.

1.3.2 Second order macroscopic models

Second order macroscopic models for traffic flow are usually composed of a set of partial differential equations of ρ and v in the following form

$$\begin{cases} \frac{\partial \rho}{\partial t} + \nabla.(\rho v) = 0, & t > 0, \quad (x, y) \in \Omega, \\ \frac{\partial v}{\partial t} + (v.\nabla)v = a(\rho, v), & t > 0, \quad (x, y) \in \Omega. \end{cases} \tag{1.2}$$

where (u, w) and (x, y) denotes the two components of v and space respectively, and

$$(v.\nabla)v = \left(u\frac{\partial u}{\partial x} + w\frac{\partial u}{\partial y}, u\frac{\partial w}{\partial x} + w\frac{\partial w}{\partial y} \right).$$

In the equation (1.2), a is the acceleration of pedestrians or vehicles that is given in terms of two unknowns. While, the first equation in (1.2) models the conservation of mass, the second one accounts for the conservation of momentum. The equation (1.2) complemented by initial conditions $\rho(0, x) = \rho_0(x), \quad v(0, x) = v_0(x)$ and, if Ω is bounded, by some boundary conditions at $\partial\Omega$ for any $t > 0$.

1.3.3 One-dimensional macroscopic models

In this subsection, we present commonly used mathematical models of one-dimensional vehicular and pedestrian dynamics.

1.3.3.1 Lighthill-Whitham-Richards (LWR) model

The conservation law for the LWR model is given by

$$\frac{\partial}{\partial t}\rho(t,x) + \frac{\partial}{\partial x}f(t,x) = 0 \tag{1.3}$$

where ρ is the vehicle or pedestrian density, f is the flux which is the product of traffic density and the traffic speed v, i.e. $f = \rho v$.
The diagram which shows the relation of dependency of the flux on traffic conditions is called *fundamental diagram*.

- **Greenshields model**
  Greenshield's model uses a linear relationship between traffic speed and traffic density, given by
  $$v(\rho) = v_{free}\left(1 - \frac{\rho}{\rho_{max}}\right) \tag{1.4}$$
  where v_{free} is the speed of traffic when the density is zero and ρ_{max} is the maximum density of traffic. The maximum density is the density at which there is a traffic jam and the speed is equal to zero.

- **Greenberg model**
  In the Greenberg model speed-density function is given by
  $$v(\rho) = v_{free}\ln\left(\frac{\rho_{max}}{\rho}\right) \tag{1.5}$$

- **Underwood model**
  In this model the velocity-density function is given by
  $$v(\rho) = v_{free}\exp\left(-\frac{\rho}{\rho_{max}}\right) \tag{1.6}$$

- **Diffusion model**
  Diffusion model is an extension of the Greenshield's model where the traffic speed depends not only on the traffic density but also on the density gradient. In this way, we model the driver's behavior where changes in traffic density in the x-direction affect the traffic speed. The model is given by
  $$v(\rho) = v_{free}\left(1 - \frac{\rho}{\rho_{max}}\right) - \frac{D}{\rho}\left(\frac{\partial\rho}{\partial x}\right) \tag{1.7}$$
  where $D = \tau v_r^2$ is a diffusion coefficient, v_r is a random velocity and τ is a relaxation parameter.

LWR models are constructed by combining different fundamental relationships between speed and density with scalar conservation law. For example, LWR model with Greenshields flow is given by

$$\frac{\partial}{\partial t}\rho(t,x) + \frac{\partial}{\partial x}v_{free}\rho\left(1 - \frac{\rho}{\rho_{max}}\right) = 0 \tag{1.8}$$

In vehicular traffic if the LWR model is used, traffic density fixes the value of traffic speed. However, in pedestrian flow, just knowing the traffic density does not fix the pedestrian speed. The actual speed depends on the function of pedestrian's movement. For example, if pedestrians are inside a museum or in a school their movement is dependent on the activity that is taking place. If however, the pedestrians are all trying to exit from a corridor, then their speed becomes a function of density just like the vehicular traffic. Notice that even in a single corridor, people could be moving in both directions at different places, but vehicular traffic on a highway or street lane is unidirectional. The models (Greenshields, Greenberg, Underwood etc.) only have to provide the speed based on density, since the direction of travel is fixed. If we introduce a time-varying scalar field that abstracts the activity that is taking place for pedestrians, we can modify the vehicular traffic model to get pedestrian models. For example LWR pedestrian model with Grenshields flow is given by

$$\frac{\partial}{\partial t}\rho + \frac{\partial}{\partial x}v_{free}(t,x)\rho\left(1 - \frac{\rho}{\rho_{max}}\right) = 0 \tag{1.9}$$

where $v_{free}(t,x) \in [-v_{max}, v_{max}]$, v_{max} is the constant maximum possible speed. We can make the free-flow speed to be the scalar control field in order to convert the LWR model with Greenshields flow into a pedestrian model. The speed of a single pedestrian would be the constant free-flow speed according to the Grenshields model. A pedestrian could be going in the positive or negative direction with the magnitude in $[0, v_{max}]$. Therefore the above choice for LWR pedestrian model is very natural one. Similar argument can be applied to the PW and AR models which will be introduced in the following subsections.

1.3.3.2 Payne-Whitham (PW) model

PW model was proposed by Payne and Whitham independently in the 1970s. In this model, partial differential equations are used to represent traffic flow. It is a second order macroscopic model. The model takes the form;

$$\begin{aligned} &\rho_t + (\rho v)_x = 0, \\ &v_t + v v_x = \frac{V(\rho) - v}{\tau} - \frac{(A(\rho))_x}{\rho} + \mu\frac{v_{xx}}{\rho}. \end{aligned} \tag{1.10}$$

where $V(\rho)$ is the equilibrium speed, τ is relaxation time, $\frac{V(\rho)-v}{\tau}$ is the relaxation term, $\frac{(A(\rho))_x}{\rho}$ is the anticipation term and $\mu\frac{v_{xx}}{\rho}$ is the viscosity term. The anticipation term is similar to the pressure term in fluids and is taken as $A(\rho) = c_0^2\rho$ for some constant c_0. In (1.10), the first equation models the conservation of mass and the second one is the fluid momentum equation.

1.3.3.3 Aw-Rascle (AR) model

The AR model that is designed to model the anisotropic traffic behavior is given by

$$\begin{aligned} \rho_t + (\rho v)_x &= 0, \\ [v + p(\rho)]_t + v[(v + p(\rho))]_x &= \frac{V(\rho) - v}{\tau}. \end{aligned} \tag{1.11}$$

where $V(\rho)$, the equilibrium speed, generally taken as Grenshields relationship. The pressure term, $p(\rho)$, is generally taken as $p(\rho) = c_0^2\rho^\gamma$, where $\gamma > 0$ and $c_0 = 1$.

1.3.4 Two-dimensional macroscopic models

In this subsection, we present two-dimensional versions of the models given in the previous subsection. The main addition in two-dimensional macroscopic models is a desired velocity vector field that makes the actual velocity follow some movement profile. These models can be used for pedestrian traffic modeling.

1.3.4.1 Two-dimensional LWR model

We consider the speed-density relationship as Grenshields for the sake of illustration. The difference of this two-dimensional model from the one-dimensional one is additional scalar field $\theta(t, x, y)$ that specifies where people move to. See the figure 1.1 for two-dimensional pedestrian traffic model. The model is given by

$$\frac{\partial}{\partial t}\rho + \frac{\partial}{\partial x}v_{free}\cos\theta\left(1 - \frac{\rho}{\rho_{max}}\right)\rho + \frac{\partial}{\partial y}v_{free}\sin\theta\left(1 - \frac{\rho}{\rho_{max}}\right)\rho = 0 \tag{1.12}$$

or in the divergence form,

$$\frac{\partial}{\partial t}\rho(t, x, y) + \nabla.q(t, x, y) = 0 \tag{1.13}$$

where

$$q = v_{max}\left(1 - \frac{\rho}{\rho_{max}}\right)\rho\begin{pmatrix}\cos\theta \\ \sin\theta\end{pmatrix} \tag{1.14}$$

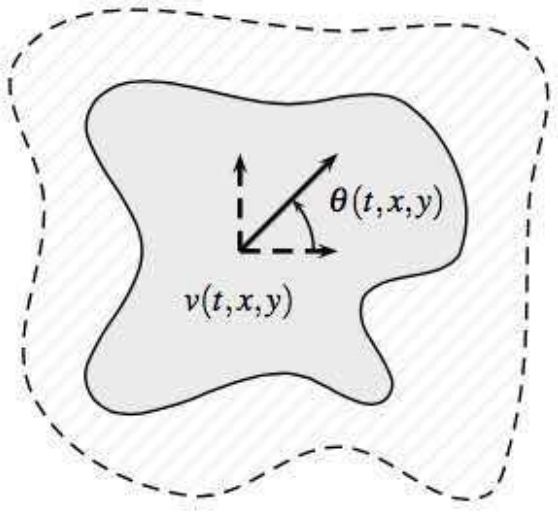

FIGURE 1.1: Pedestrian flow in two-dimensions

1.3.4.2 Two-dimensional PW model

We propose a viscous two-dimensional version of the Payne-Whitham model suitable for pedestrian modeling. In the equations, u stands for the x-component and w for the y-component of velocity, i.e. $v = (u, w)$. The anticipation term remains the same as it represents isotropic traffic pressure.

$$\begin{aligned} &\rho_t + (\rho u)_x + (\rho w)_x = 0, \\ &u_t + uu_x + uu_y = \frac{V_1(t,x,y,\rho) - u}{\tau} - \frac{(A(\rho))_x}{\rho} + \mu\left(\frac{u_{xx}}{\rho} + \frac{u_{yy}}{\rho}\right), \\ &w_t + ww_x + ww_y = \frac{V_2(t,x,y,\rho) - w}{\tau} - \frac{(A(\rho))_y}{\rho} + \mu\left(\frac{w_{xx}}{\rho} + \frac{w_{yy}}{\rho}\right). \end{aligned} \tag{1.15}$$

where

$$V_1(t,x,y,\rho) = v_{free}\cos\theta\left(1 - \frac{\rho}{\rho_{max}}\right), \quad V_2(t,x,y,\rho) = v_{free}\sin\theta\left(1 - \frac{\rho}{\rho_{max}}\right).$$

The anticipation term is taken as $A(\rho) = c_o^2\rho$.

1.3.4.3 Two-dimensional AR model

We give the formulation for two-dimensional version of the Aw-Rascle model with relaxation terms suitable for pedestrian modeling. The relaxation terms are modified so that $v_{max}(t,x,y)$ and $\theta(t,x,y)$ scalar fields can enter the dynamics to affect the pedestrian

movement.

$$\begin{aligned} \rho_t + (\rho u)_x + (\rho w)_x &= 0, \\ [u + p(\rho)]_t + u[(u + p(\rho))]_x + w[(u + p(\rho))]_y &= \frac{V_1(t, x, y, \rho) - u}{\tau}, \\ [w + p(\rho)]_t + u[(w + p(\rho))]_x + w[(w + p(\rho))]_y &= \frac{V_2(t, x, y, \rho) - w}{\tau}. \end{aligned} \tag{1.16}$$

where

$$V_1(t, x, y, \rho) = v_{free} \cos\theta \left(1 - \frac{\rho}{\rho_{max}}\right), \quad V_2(t, x, y, \rho) = v_{free} \sin\theta \left(1 - \frac{\rho}{\rho_{max}}\right),$$

and $v = (u, w)$.

1.4 Thesis layout

The thesis is composed of five chapters. The first chapter is an introduction to mathematical models for collective behavior. We introduced most commonly used mathematical models for traffic flow both for vehicular and pedestrian dynamics. They fall into two main category; microscopic and macroscopic models. Since the main work deals with a macroscopic model for pedestrian flow, we did not go into details of microscopic models. We explained one-dimensional and two-dimensional versions of three macroscopic mathematical models for traffic flow. They are known as Lighthill-Whitham-Richards (LWR) model, Payne-Whitham (PW) model and Aw-Rascle (AR) model.

In the second chapter, we present the Hughes' model describing the equations of motion governing two-dimensional flow of pedestrians of both single and multiple pedestrian types. The model proposed by Roger L. Hughes [6, 7]. Hughes' model develops a theoretical framework for understanding the mechanics of pedestrian dynamics especially in large crowds. In the first two sections, we introduce the Hughes' model for the flow of pedestrians of single and multiple types. Then, we give the definition of one-dimensional version of Hughes' model along with initial and boundary conditions. Some properties of solutions are also derived. The study is based on [1, 10].

In the third chapter, we explain non-local version of the Lighthill-Whitham-Richards (LWR) model ([2, 5, 8]) for traffic flow. We define the problem with initial and boundary conditions and we present numerical solution to it constructed by using Lax-Friedrichs numerical scheme.

In the fourth chapter, we give simulations of one dimensional Hughes'model both the original and the non-local version. We used the fast sweeping method to solve eikonal equation. A finite volume scheme with Rusanov flux is used to solve the continuity

equation numerically. We followed and improved the work [4, 5]. For the numerical solution of non-local version of Hughes' model, both Gaussian and rectangular convolution kernels are considered in order to include effects of local density change. We present the solutions and evacuation times changing with the smoothness degree of the model.
In the last chapter, we discuss future work and possible extensions, improvements of the numerical schemes used in the project.

Chapter 2

The Hughes' model for pedestrian flow

In this chapter, we introduce the Hughes' model for pedestrian flow. The study of a human crowd as a moving fluid is a recent topic of research. The main difference of a crowd in motion and a moving fluid is that the crowd has ability to decide its own way. Roger L. Hughes [6, 7] derived the equations of motion governing the two-dimensional flow of pedestrians of both single and multiple pedestrian types.

There are two separate approaches to follow while modeling crowd dynamics. The first approach involves treating each pedestrian individually in a discrete manner following them walking through the domain in a computer simulation. Pedestrians can be modeled using a granular material behavior. It is assumed that the pedestrians will try to optimize their immediate local behavior while moving along predefined globally determined paths. The second approach involves treating the crowd as a whole. It can be applicable only to large crowds. Crowds are considered either as a fluid or a continuum responding to local influences or it is assumed that individuals in the continuum move by optimizing their behavior in order to achieve non-local objectives. Whereas the former approach is more appropriate for small crowds, the latter gives us a better understanding of the rules governing the overall behavior of the flow.

Hughes' model develops a theoretical framework for understanding the mechanics of pedestrian dynamics especially in large crowds. In the first two sections of this chapter we introduce the Hughes' model for the flow of pedestrians of single type and of multiple type. Then in the last section, we present the one-dimensional version of Hughes' model.

2.1 Hughes' model for the flow of pedestrians of single pedestrian type

In the Hughes' model, a pedestrian flow, in which only one type of pedestrian is considered, is described in terms of two quantities.
(i) density of the flow, ρ, is defined as the expected number of individuals located within unit area at a given time t and location (x, y).
(ii) velocity of the flow, (u, w), is defined as the expected velocity of individuals at a given time t and location (x, y).
Therefore, by equating the net flow of pedestrians into a small region to the time rate of accumulation of pedestrians in the region and letting the area of the region shrink to zero, conservation of pedestrians implies

$$\frac{\partial \rho}{\partial t} + \frac{\partial}{\partial x}(\rho u) + \frac{\partial}{\partial y}(\rho w) = 0 \tag{2.1}$$

This equation is known as the *continuity equation* in fluid mechanics.
There are three hypotheses made in Hughes' model about the pedestrian motion.
Hypothesis 1. The walking speed of the pedestrians determined merely by the density of surrounding pedestrians, their behavioral characteristics and the ground on which they walk.
The velocity components (u, w) of a single pedestrian is given by

$$u = v(\rho)\hat{\phi}_x, \qquad w = v(\rho)\hat{\phi}_y \tag{2.2}$$

where ϕ_x and ϕ_y are the direction cosines of the motion and $v(\rho)$ is the speed of the pedestrian as a function of density. Here in this model, the density is preferably high but not extreme and the speed of a pedestrian $v(\rho)$ is determined in a similar manner with the Greenshields relation (1.4) which uses a linear relationship between the density and the speed. However, there is not any uniformly accepted form of the function $v(\rho)$ which relates the density and the speed since it depends on many factors related with the situation of the pedestrians and the ground on which they are walking. But this assumption is essential to be able to use the LWR model (1.9) for conservation of pedestrians.
Hypothesis 2. Pedestrians have a common sense of the task (called potential) that they face to reach their common destination, such that any two individuals at different locations having the same potential would see no advantage of exchanging their positions. So, the direction of a motion of the pedestrian is perpendicular to his potential, i.e. the

direction of cosines are

$$\hat{\phi}_x = \frac{-\frac{\partial\phi}{\partial x}}{\sqrt{(\frac{\partial\phi}{\partial x})^2 + (\frac{\partial\phi}{\partial y})^2}}, \qquad \hat{\phi}_y = \frac{-\frac{\partial\phi}{\partial y}}{\sqrt{(\frac{\partial\phi}{\partial x})^2 + (\frac{\partial\phi}{\partial y})^2}} \tag{2.3}$$

where ϕ is the potential. This hypothesis is applicable to pedestrian flow if pedestrians can visually access the situation. In this case, it must be assumed also that shorter pedestrians set their direction according to taller pedestrians in the crowd since the taller pedestrians have the overall view of the situation.

Hypothesis 3. Pedestrians seek to minimize their estimated travel time but temper this behavior to avoid extreme densities. This tempering is assumed to be separable, such that pedestrians minimize the product of their travel time as a function of density. This hypothesis claims that the distance between potentials of two pedestrians must be proportional to pedestrian speed independent on the initial position of a pedestrian since two pedestrians on a given potential must both be at the same new potential as each other at some later time. So, we write

$$\frac{1}{\sqrt{(\frac{\partial\phi}{\partial x})^2 + (\frac{\partial\phi}{\partial y})^2}} = g(\rho)\sqrt{u^2 + w^2} \tag{2.4}$$

where ϕ is the potential which has been scaled appropriately and $g(\rho)$ stands for the tempering behavior at high densities. $g(\rho)$ is taken to be unity in general and it increases for high densities.

Equations (2.1), (2.2), (2.3) and (2.4) combine to form the governing equations for pedestrian flow

$$-\frac{\partial\rho}{\partial t} + \frac{\partial}{\partial x}\Big(\rho g(\rho)v^2(\rho)\frac{\partial\phi}{\partial x}\Big) + \frac{\partial}{\partial y}\Big(\rho g(\rho)v^2(\rho)\frac{\partial\phi}{\partial y}\Big) = 0 \tag{2.5a}$$

$$g(\rho)v(\rho) = \frac{1}{\sqrt{(\frac{\partial\phi}{\partial x})^2 + (\frac{\partial\phi}{\partial y})^2}} \tag{2.5b}$$

Although most of the situations can be described by the equations (2.5a) and (2.5b), it is needed to specify the boundary conditions for every particular situation. In general, ρ is defined on open boundaries corresponding to entrances. We automatically get the flux, $\rho v(\rho)$, by specifying the density, ρ, and the speed, $v(\rho)$. The potential, ϕ, is zero on exits and the normal derivative of the potential is taken as zero on the closed boundaries. Morever, depending on the particular situations such as queuing of smaller crowds, it is sometimes necessary to assume additional hypotheses and to modify the above hypotheses. In the original paper, these are called as *local hypotheses* and *local modifications*.

In order to study properties of solutions we define the flow of pedestrians per unit width,

f, by

$$f(\rho) = \rho v(\rho) \tag{2.6}$$

The functions, $v(\rho)$ and $g(\rho)$ must satisfy the following properties;

$$\begin{aligned} &(i) \quad v(0) \quad \text{is finite}, \quad (ii) \quad v(\rho_{max}) = 0, \quad (iii) \quad \frac{dv(\rho)}{d\rho} \leq 0, \\ &(iv) \quad g(\rho) \geq 1, \quad (v) \quad \frac{dg(\rho)}{d\rho} \geq 0. \end{aligned} \tag{2.7}$$

where ρ_{max} is the density at which pedlock occurs. The function $g(\rho)$ has been chosen as unity in general. For the function $v(\rho)$, there are several forms proposed in the literature. We take it as linear similar to Greenshields (1.4),

$$v(\rho) = A - B\rho \tag{2.8}$$

where A and B are positive constants. By (2.6) and (2.8), the flux f becomes;

$$f(\rho) = \rho(A - B\rho) \tag{2.9}$$

so that it has the maximum value of $A^2/4B$ at $\rho = A/2B$. If the flow is less than the maximum at a time, there are two possible states of the speed of pedestrians in the flow. One of them is high speed of the flow in the low-density region, called *supercritical flow*, and the other one is low speed of the flow in the high-density region, called *subcritical flow*.

We consider the equations (2.5a) and (2.5b) at low flows in order to see the effects of supercritical and subcritical flows. In the case of a supercritical flow, spatial variations of the potential ϕ are negligible compared to the variations of ϕ in ρ. So the steady-state form of (2.5a) takes the form;

$$\frac{\partial \rho}{\partial x}\frac{\partial \phi}{\partial x} + \frac{\partial \rho}{\partial y}\frac{\partial \phi}{\partial y} \approx 0. \tag{2.10}$$

The equation (2.10) implies that lines of constant density is almost perpendicular to lines of constant potential. The density of the flow varies slowly in the direction of the flow.

For the subcritical flow, spatial variations in ρ are negligible compared to those in ϕ. So the equation (2.5a) takes the form of Laplace's equation.

$$\frac{\partial^2 \phi}{\partial x^2} + \frac{\partial^2 \phi}{\partial y^2} \approx 0. \tag{2.11}$$

The equation (2.11) is solvable numerically by using some techniques.

2.2 Extension of Hughes' model to multiple pedestrian types

In the section 2.1 the partial differential equations describing the flow of pedestrians of a single type were introduced. There are three hypotheses made about the nature of movements of pedestrians. In reality, instead of consisting in a single type of pedestrians, crowds are composed of multiple pedestrian types depending on the differences of walking styles and destinations of pedestrians. In this section, the extension of Hughes' model to this type of pedestrian flow is discussed by stating three hypotheses.

Hypothesis 1A. The speed of pedestrians of a single type in multiple type flow is determined by the function $v(\rho)$ where ρ is the total density not the density of a single pedestrian type.

There are many observations and studies supporting this hypothesis in the literature. Moreover, this hypothesis is supplemented by the following two hypotheses similar to the ones in the previous section.

Hypothesis 2A. A potential field exists for each pedestrian type such that pedestrians move at right angles to lines of constant potential.

Hypothesis 3A. Pedestrians look for the path which minimizes their estimated travel time. But they may alter this path in order to avoid extreme densities.

Thus, the flow of a particular type of pedestrians, type i, is given by $\rho_i v(\rho_i)$ where ρ_i is the density of pedestrians of particular type and $v(\rho_i)$ is a specified function of total pedestrian density for pedestrians of type i. Moreover, the following equality holds,

$$\rho = \sum_{i=1}^{N} \rho_i \tag{2.12}$$

where N is the number of pedestrian types. The governing equations for each type of pedestrians i is given by;

$$-\frac{\partial \rho_i}{\partial t} + \frac{\partial}{\partial x}\left(\rho_i g(\rho) v_i^2(\rho) \frac{\partial \phi_i}{\partial x}\right) + \frac{\partial}{\partial y}\left(\rho_i g(\rho) v_i^2(\rho) \frac{\partial \phi_i}{\partial y}\right) = 0 \tag{2.13a}$$

$$g(\rho) v_i(\rho) = \frac{1}{\sqrt{(\frac{\partial \phi_i}{\partial x})^2 + (\frac{\partial \phi_i}{\partial y})^2}}, \quad i = 1, ..., N. \tag{2.13b}$$

where ϕ_i is the potential for type i of pedestrian.

2.3 The one-dimensional Hughes' model for pedestrian flow

In this section we define the one-dimensional version Hughes' model for pedestrian flow, analyze its solutions and some properties of solutions. The problem (2.15) presents a nontrivial coupling between a scalar conservation law and an eikonal equation. It poses some challenging questions about existence, uniqueness and numerical approximation of solutions. Following the previous study done in [1, 4] we present solutions to one-dimensional Hughes' model and mention some properties of these solutions. By omitting the y-space variable from the equations (2.5a) and (2.5b) and taking the tempering factor $g(\rho)$ as unity we generalize Hughes' model for pedestrian flow in one space dimension as,

$$\begin{aligned} -\frac{\partial \rho}{\partial t} + \frac{\partial}{\partial x}\Big(\rho v^2(\rho)\frac{\partial \phi}{\partial x}\Big) &= 0, \\ v(\rho) &= \frac{1}{\left|\frac{\partial \phi}{\partial x}\right|}, \end{aligned} \tag{2.14}$$

We shorten the notation as following,

$$\begin{aligned} \rho_t - (\rho v^2(\rho)\phi_x)_x &= 0, \\ v(\rho)|\phi_x| &= 1. \end{aligned} \tag{2.15}$$

Here we take $x \in \Omega :=]-1, 1[$ and the mean velocity as $v(\rho) = 1 - \rho$. So the initial-boundary value problem takes the form

$$\rho_t - (\rho v^2(\rho)\phi_x)_x = 0, \quad x \in \Omega, \quad t \geq 0, \tag{2.16a}$$

$$v(\rho)|\phi_x| = 1, \quad x \in \Omega, \quad t \geq 0, \tag{2.16b}$$

$$\rho(0, x) = \rho_0(x) \in [0, 1] \quad x \in \Omega, \tag{2.16c}$$

$$\phi(t, -1) = \phi(t, 1) = 0, \quad t \geq 0. \tag{2.16d}$$

where (2.16c) is the initial condition and (2.16d) is the boundary condition. We denote the flux as $f(\rho) = \rho v(\rho)$ and we assume $f \in C^2([0, 1]), \quad f'' < 0, \quad f(0) = 1, \quad f(1) = 0,$ and f is strictly concave. We denote the unique point in $(0, 1)$ where f has its maximum as $\bar{\rho}$. Then, at the boundaries ± 1 we require that

$$Tr\rho(t, .) \in [0, \bar{\rho}], \quad x = \pm 1, \quad t \geq 0. \tag{2.17}$$

The flux in (2.16) can be written as

$$\rho v^2(\rho)\phi_x = \rho v(\rho) sgn\phi_x = f(\rho) sgn\phi_x.$$

Then, the zero-Dirichlet boundary condition can be stated as in the [1],

$$\min_{k\in[0,Tr\rho]}\{-(f(Tr\rho)sgn\phi_x(t,x)+f(k)sgn\phi_x(t,x))sgn(x)\}=0, \quad x=\pm 1 \tag{2.18}$$

since the eikonal equation in (2.16b) will be solved in the semi-concave sense in the following subsection 2.3.1, we write $\phi_x(-1,t)>0$ and $\phi_x(1,t)<0$. Thus, (2.18) becomes

$$\min_{k\in[0,Tr\rho]}\{f(Tr\rho)-f(k)=0\}, \quad x=\pm 1,$$

so that we can write the boundary condition (2.17) as it is.

2.3.1 Solution for the eikonal equation

In this subsection we solve the eikonal equation (2.16b) and accordingly restate the initial-boundary value problem (2.16).
Let us assume that the density $\rho(t,.)$ is known in (2.16b) and further assume that $\rho(t,x)\in[0,1-\delta]$ for all $x\in\Omega, \quad t\geq 0$ for some $\delta>0$ so that we can write (2.16b) as

$$|\phi_x|=\frac{1}{v(\rho)}:=c(\rho) \tag{2.19}$$

and ϕ is a globally Lipschitz function on $[0,1]$.
We assume that the cost function $c:[0,1]\to[1,+\infty]$ is a smooth function such that $c(0)=1$ and $c'(\rho)\geq 0$.
Solutions of the equation (2.19) are the points in Ω in which ϕ_x changes its sign. According to the theory of Hamilton-Jacobi equations there may be more than one, in fact infinitely may solutions (e.g. $1/v(\rho)$ is a constant) but we look for a unique point, ξ, such that $\phi_x>0$ in $]-1,\xi]$ and $\phi_x<0$ in $[\xi,1[$. Following [1], the unique solution ϕ of (2.19) can be found in such a way that ϕ_{xx} is bounded from above in the sense of distributions which are called *semi-concave solutions* for (2.19).
The physical interpretation of the solution ϕ for (2.19) as follows. Since the boundary points $x=\pm 1$ are the targets, it is reasonable to expect that the potential ϕ will increase close to $x=-1$ and decrease close to $x=1$ as pedestrians will choose to go to boundary points if they are close to them. But we need to show that ϕ_x will change its sign in the interval $]-1,1[$ only once. We assume for a contradiction that, for a given ρ, following condition holds:

$$\phi_x(x_1)>0, \quad \phi_x(x_2)<0, \quad \phi_x(x_3)>0, \quad \textit{and} \quad x_1<x_2<x_3.$$

The pedestrians are located as in the figure 2.1. But this is a contradiction since the pedestrian located in x_2 cannot see the exit at $x=1$ if the pedestrian located at x_3

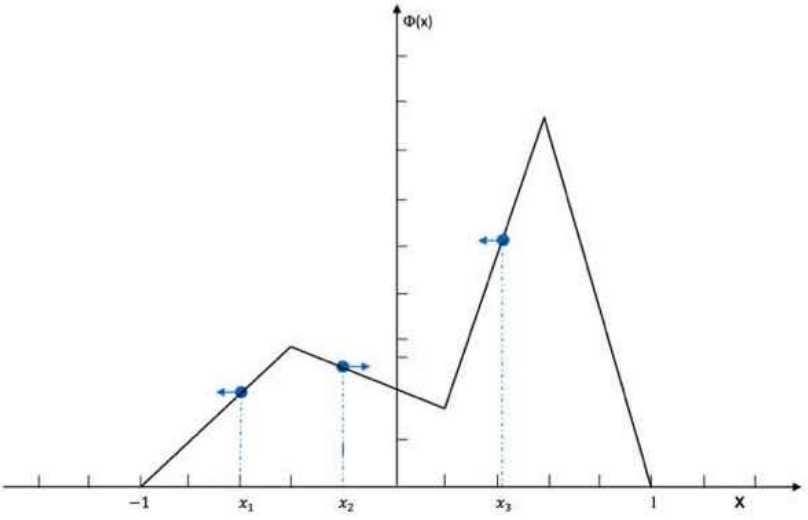

FIGURE 2.1: Pedestrians are located at x_1, x_2 and x_3. Arrows show the direction of the exits which pedestrians take

cannot sense it since x_3 is closer to the exit at $x = 1$ than the point x_2. Thus, by this contradiction we deduce that there must be a unique point, called *turning point*, $\xi(t)$, at which ϕ_x changes its sign, i.e.

$$\phi_x(t,x) > 0 \quad if \quad -1 < x < \xi(t), \qquad \phi_x(t,x) < 0 \quad if \quad \xi(t) < x < 1. \tag{2.20}$$

Then we can rewrite the conservation law (2.16) as

$$\rho_t - (f(\rho))_x = 0, \quad -1 < x < \xi(t), \tag{2.21}$$

$$\rho_t + (f(\rho))_x = 0, \quad \xi(t) < x < 1. \tag{2.22}$$

Thus, when we know that there exists a turning point, we can explicitly solve the eikonal equation (2.16b) with the boundary condition (2.16d) as follows,

$$\phi(t,x) = \begin{cases} \int_{-1}^{x} c(\rho(t,y))dy & -1 < x < \xi(t), \\ \int_{x}^{1} c(\rho(t,y))dy & \xi(t) < x < 1. \end{cases} \tag{2.23}$$

Since ϕ is continuous, for the turning point $\xi(t)$ we can write;

$$\int_{-1}^{\xi(t)} c(\rho(t,y))dy = \int_{\xi(t)}^{1} c(\rho(t,y))dy. \tag{2.24}$$

Since $v > 0$ on $[0,1)$, then $\xi(t)$ is uniquely determined.
It has been clarified from the formula (2.24) that the turning point $\xi(t)$ depends *non-locally* on the distribution of pedestrians $\rho(t)$ on Ω. So, it can be determined by using

the initial datum ρ_0 at $t = 0$ by the following formula;

$$\int_{-1}^{\xi(0)} c(\rho_0(y))dy = \int_{\xi(0)}^{1} c(\rho_0(y))dy. \tag{2.25}$$

There are several results and studies about the proof of existence of a unique solution for Hamilton-Jacobi type equations with discontinuous coefficients under appropriate compatibility conditions. Since it is not the main aim of this work, we leave it to the reader by saying that in our problem, $\rho(t,.)$ being a function of bounded variation is enough condition to have a unique solution.

2.3.2 Some properties of solutions

The equation (2.16) can be written as a scalar conservation law with discontinuous space-time dependent flux:

$$\rho_t + F(t,x,\rho)_x = 0, \tag{2.26}$$

where $F(t,x,\rho) = sgn(x-\xi(t))f(\rho)$. Thus, the initial-boundary value problem takes its simplest form as,

$$\begin{aligned} \rho_t + F(t,x,\rho)_x = 0, \quad x \in \Omega, \quad t \geq 0, \\ |\phi_x| = c(\rho), \quad x \in \Omega, \quad t \geq 0, \\ \rho(0,x) = \rho_0(x), \quad x \in \Omega, \\ \rho(t,-1) = \rho(t,1) = 0, \quad \phi(t,-1) = \phi(t,1) = 0, \quad t \geq 0. \end{aligned} \tag{2.27}$$

We state some properties of solutions of (2.27) by following [1, 4, 10].

Definition 1. A solution $\rho \in \mathbf{L}^\infty(\mathbb{R}^+ \times \Omega)$ of the initial-boundary value problem (2.27) is a *weak solution* if for every $\varphi \in \mathbf{C}_c^\infty(\mathbb{R} \times \Omega)$ the following equality holds:

$$\int_0^{+\infty} \int_{-1}^{1} (\rho\varphi_t + F(t,x,\rho)\varphi_x)dxdt + \int_{-1}^{1} \rho_0(x)\varphi(0,x)dx = 0. \tag{2.28}$$

Moreover if we assume that $\rho \in \mathbf{C}^0(\mathbb{R}^+; BV(\Omega) \cap \mathbf{L}^1(\Omega))$, ρ is a weak solution of (2.27) if and only if it satisfies in the weak sense

$$\begin{aligned} \rho_t - (f(\rho))_x = 0, \quad x \in]-1, \xi(t)[, \quad t > 0, \\ \rho_t + (f(\rho))_x = 0, \quad x \in]\xi(t), 1[, \quad t > 0, \\ \rho(0,x) = \rho_0(x), \quad x \in \Omega, \end{aligned} \tag{2.29}$$

where $\xi(t) \in \mathbf{C}^0(\mathbb{R}^+)$ which is implicitly defined by (2.24). The Rankine-Hugoniot condition

$$f(\rho^+) + f(\rho^-) = \xi'(t)(\rho^+ - \rho^-) \tag{2.30}$$

holds where $\rho^+ = \rho^+(t) = \rho(t, \xi(t)+)$ and $\rho^- = \rho^-(t) = \rho(t, \xi(t)-)$ the right and left traces of ρ at $x = \xi(t)$.

Remark that if $\rho(t, .)$ is continuous at $x = \xi(t)$ then (2.30) gives $f(\rho(t, \xi(t))) = 0$ and therefore $\rho(t, \xi(t)) \in \{0, 1\}$. Moreover, if $\rho(t, \xi(t)) = 1$, we have $sgn(x - \xi(t))f'(\rho) < 0$ and thus we have $\| \rho_0 \|_{\mathbf{L}^\infty(\Omega)} = 1$.

Definition 2. A weak solution ρ of the initial-boundary value problem (2.27) is an *entropy weak solution* if the following Kružkov-type entropy inequality holds for all $k \in \mathbb{R}$ and for all test functions $\varphi \in \mathbf{C}_c^\infty(\mathbb{R} \times \Omega), \varphi \geq 0$,

$$\begin{aligned} 0 \leq \int_0^{+\infty} \int_{-1}^{1} (|\rho - k|\varphi_t + sgn(\rho - k)(F(t, x, \rho) - F(t, x, k))\varphi_x) dx dt + \int_{-1}^{1} |\rho_0(x) - k|\varphi(0, x) dx \\ + sgn(k) \int_0^{+\infty} (f(\rho(t, 1-)) - f(k))\varphi(t, 1) dt + sgn(k) \int_0^{+\infty} (f(\rho(t, -1+)) - f(k))\varphi(t, -1) dt \\ + 2 \int_0^{+\infty} f(k)\varphi(t, \xi(t)) dt. \end{aligned} \tag{2.31}$$

The entropy boundary condition used here implies $\rho(t, \mp 1\pm) \leq 1/2$.

Corollary 1. Let $\rho \in \mathbf{C}^0(\mathbb{R}^+; BV(\Omega) \cap \mathbf{L}^1(\Omega))$ be an entropy-weak solution in the sense of **Definition 2**, then the following *entropy jump condition* must hold for all $k \in \mathbb{R}$ and a.e. $t \in \mathbb{R}^+$,

$$\begin{aligned} sgn(\rho^+(t) - k)(f(\rho^+(t)) - f(k)) - \xi'(t)|\rho^+(t) - k| \\ + sgn(\rho^-(t) - k)(f(\rho^-(t)) - f(k)) - \xi'(t)|\rho^-(t) - k| \leq 2f(k). \end{aligned} \tag{2.32}$$

Remark 1. If we take $k \leq \rho^-$ and $k \leq \rho^+$ we get

$$f(\rho^+) + f(\rho^-) \leq 4f(k) + \xi'(t)(\rho^+ - \rho^-). \tag{2.33}$$

If we take $k \geq \rho^-$ and $k \geq \rho^+$ we obtain

$$f(\rho^+) + f(\rho^-) \geq \xi'(t)(\rho^+ - \rho^-). \tag{2.34}$$

Note that we recover the Rankine-Hugoniot condition (2.30) by taking $k = 0$ in the inequalities (2.33) and (2.34). So, for k between ρ^- and ρ^+ we obtain

$$sgn(\rho^+ - \rho^-)[f(\rho^+) - f(\rho^-) + \xi'(t)(2k - \rho^+ - \rho^-)] \leq 2f(k). \tag{2.35}$$

Proposition 1. Let $\rho \in \mathbf{C}^0(\mathbb{R}^+; BV(\Omega) \cap \mathbf{L}^1(\Omega))$ be an entropy-weak solution in the sense of **Definition 2** and assume $\rho^+(t) \neq \rho^-(t)$. Then the characteristic speeds at $x = \xi(t)$ must enter the switch curve $x = \xi(t)$ on the side of higher density, i.e.

$$\begin{aligned} f'(\rho^+(t)) \leq \xi'(t), \quad if \quad \rho^-(t) < \rho^+(t), \\ -f'(\rho^-(t)) \geq \xi'(t), \quad if \quad \rho^-(t) > \rho^+(t). \end{aligned}$$

Proof. We multiply (2.35) and use (2.30) we obtain that

$$f(\rho^+)(k - \rho^-) - f(\rho^-)(\rho^+ - k) \leq f(k)|\rho^+ - \rho^-|. \tag{2.36}$$

For $\rho^- \leq k \leq \rho^+$ we get from (2.36) that

$$\frac{f(\rho^+) - f(k)}{\rho^+ - k} \leq \frac{f(k) + f(\rho^-)}{k - \rho^-}.$$

Then we let $k \nearrow \rho^+$ and using (2.30) we obtain $\xi'(t) \geq f'(\rho^+(t))$. So, the characteristic lines are entering the sign change line $x = \xi(t)$ on the right hand side.
For $\rho^+ \leq k \leq \rho^-$ we get from (2.36) that

$$\frac{f(\rho^-) - f(k)}{\rho^- - k} \leq \frac{f(k) + f(\rho^+)}{k - \rho^+}.$$

Then we let $k \nearrow \rho^-$ and using (2.30) we obtain $\xi'(t) \leq -f'(\rho^-(t))$. So, the characteristic lines are entering the sign change line $x = \xi(t)$ on the left hand side.
The definition of entropy weak solution implies that the traces at $x = \xi(t)$ must satify the bounds $0 \leq \rho(t+, \xi(t+)\pm) \leq \sup\{\rho(t, y) : y \in \Omega\}$. Combining this with $\| \rho_0 \|_{\mathbf{L}^\infty(\Omega)} = 1$ we deduce the following Corollary.
Corollary 2. Let $\rho \in \mathbf{C}^0(\mathbb{R}^+; BV(\Omega) \cap \mathbf{L}^1(\Omega))$ be an entropy weak solution of (2.27), then

$$0 \leq \rho(t, x) \leq \| \rho_0 \|_{\mathbf{L}^\infty(\Omega)}.$$

By the above maximum principle, we can avoid blow up in cost function $c(\rho) = 1/v(\rho)$ by taking initial data $\rho_0(x) \in [0, 1 - \delta]$, for $\delta > 0$.
Moreover, under certain assumptions on initial data and some hypotheses, solution to the Riemann problem around the turning point can completely be determined and it is self-similar. For more details we refer to [1, 2].

Chapter 3

The Lighthill-Whitham-Richards traffic flow model with non-local velocity

In the chapter 2, we analyzed a macroscopic model for pedestrian dynamics which is proposed by Roger L. Hughes. According to the governing equations (2.5a)-(2.5b) of the Hughes' model, individuals try to minimize their travel time while avoiding the high-density regions. But one of the important assumptions of the Hughes' model for flow of pedestrians is that the overall density of the crowd is known by every individual. Moreover, all walking costs of individuals are based on the current density. But the assumption of complete and continuous knowledge of the overall density is not practical in real-world applications. Thus, by this motivation, modified versions of the macroscopic traffic flow models such as LWR (1.3) and Hughes (2.5) based on partial knowledge of the overall density became a recent topic of research. These models account for the reaction of drivers or pedestrians to the surrounding density of other individuals. Although interpretation and implementation of such models in microscopic level is intuitive, their translation to macroscopic models is quite complicated. Non-local effects of macroscopic models for traffic flow often interpreted as the deviation of the crowd from the desired direction. This deviation is determined by the average density perceived by the vehicles or pedestrians and it is modeled by a convolution operator acting on the velocity term. In this chapter, we will present a classical LWR traffic flow model [2, 5], in which the mean velocity is assumed to be dependent on the downstream traffic density.

3.1 Definition and well-posedness of the model

Following [2], we write the mass conservation equation for traffic flow with non-local mean velocity as follows;

$$\partial_t \rho(t,x) + \partial_x \Big(\rho(t,x) v(\int_x^{x+\eta} \rho(t,y) w_\eta(y-x) dy) \Big) = 0, \tag{3.1}$$

where $t \in \mathbb{R}^+$, $x \in \mathbb{R}$ and $\eta > 0$. In the above equation, convolution kernel $w_\eta \in C^1([0,\eta];\mathbb{R}^+)$ is taken as a non-increasing function satisfying the following condition

$$\int_0^\eta w_\eta(x) dx = 1.$$

In this model, it is considered that the drivers will change their velocity according to the downstream traffic. They will react to what happens in front on them by adapting their density with respect to the downstream density. Such behavior is modeled by the downstream convolution product as follows;

$$\rho *_d w_\eta(t,x) = \int_x^{x+\eta} \rho(t,y) w_\eta(y-x) dy. \tag{3.2}$$

We take the velocity $v(\rho) = 1 - \rho$ as before and we set $V(t,x) = v(\rho *_d w_\eta(t,x))$ so that the governing equations for traffic flow takes the form

$$\partial_t \rho(t,x) + \partial_x(\rho(t,x) V(t,x)) = 0, \tag{3.3}$$

$$\rho(0,x) = \rho_0(x) \in BV(\mathbb{R};[0,1]). \tag{3.4}$$

In [5], the velocity function is taken as a general continuous function instead of the specific case $v(\rho) = 1 - \rho$. But mainly we follow [2] here.
We consider $\rho(t,x)$ satisfying the following definitions;
Definition 1. A function $\rho \in (\mathbf{L}^1 \cap \mathbf{L}^\infty \cap BV)(\mathbb{R}^+ \times \mathbb{R};[0,1])$ is a *weak solution* of (3.3) and (3.4) if

$$\int_0^{+\infty} \int_{-\infty}^{+\infty} (\rho \varphi_t + \rho(t,x) v(\rho *_d w_\eta) \varphi_x) dx dt + \int_{-\infty}^{+\infty} \rho_0(x) \varphi(0,x) dx = 0 \tag{3.5}$$

for all $\varphi \in \mathbf{C}_c^1(\mathbb{R}^2;\mathbb{R})$.
Definition 2. A function $\rho \in (\mathbf{L}^1 \cap \mathbf{L}^\infty \cap BV)(\mathbb{R}^+ \times \mathbb{R};[0,1])$ is an *entropy weak solution*

if

$$\int_0^{+\infty}\int_{-\infty}^{+\infty}(|\rho-k|\varphi_t+|\rho-k|V\varphi_x-sgn(\rho-k)kV_x\varphi)(t,x)dxdt + \int_{-\infty}^{+\infty}|\rho_0(x)-k|\varphi(0,x)dx\geq 0. \quad (3.6)$$

for all $\varphi\in\mathbf{C}_c^1(\mathbb{R}^2;\mathbb{R})$ and $k\in\mathbb{R}$.

Remark that the assumptions of Kružkov are not fully satisfied since the convolution kernel ω_η is not continuous on $\mathbb{R}$. Therefore, the uniqueness of the entropy weak solutions is not guaranteed. Following theorem is the main result of the work [2].

Theorem 1. Let $\rho_0\in BV(\mathbb{R};[0,1])$ and $\omega_\eta\in\mathbf{C}^1([0,\eta];\mathbb{R})$ be a non-increasing function such that $\int_0^\eta\omega_\eta(x)dx=1$. Then the Cauchy problem

$$\begin{cases}\partial_t\rho+\partial_x(\rho v(\rho *_d \omega_\eta))=0, & x\in\mathbb{R}, t>0,\\ \rho(0,x)=\rho_0(x), & x\in\mathbb{R},\end{cases}$$

admits a weak solution in the sense of **Definition 1** and **Definition 2**, such that

$$\min_{\mathbb{R}}\{\rho_0\}\leq\rho(t,x)\leq\max_{\mathbb{R}}\{\rho_0\},\quad for\quad a.e.\quad x\in\mathbb{R}, t>0. \quad (3.7)$$

The existence of a weak entropy solution is proved by constructing a converging sequence of finite volume approximate solutions, defined using an adapted Lax-Friedrichs scheme. This method does not require the convolution kernel ω_η to be smooth. In the next sections, the description of the finite volume scheme used to construct approximate solutions is given and its some properties are stated along with their proofs.

3.2 A Lax-Friedrichs numerical scheme

We start by taking a space step Δx such that $\eta=N\Delta x$, for some $N\in\mathbb{N}$, and a time step Δt satisfying the Courant–Friedrichs–Lewy (CFL) conditions which will be specified later. For $j\in\mathbb{Z}$ and $n\in\mathbb{N}$, let $x_{j+1/2}=j\Delta x$ be the cells interfaces, $x_j=(j-\frac{1}{2})\Delta x$ the cells centers and $t^n=n\Delta t$ the time mesh. We construct a finite volume approximate solution $\rho_{\Delta x}(t,x)=\rho_j^n$ for $(t,x)\in C_j^n=[t^n,t^{n+1}[\times]x_{j-1/2},x_{j+1/2}[$. Given the piece-wise constant approximation of the initial datum ρ_0,

$$\rho_j^0=\frac{1}{\Delta x}\int_{x_{j-1/2}}^{x_{j+1/2}}\rho_0(x)dx,$$

and denoting $\omega_\eta^k := \omega_\eta(k\Delta x)$ for $k = 0, 1, ..., N-1$, we set

$$V_j := v\Big(\Delta x \sum_{k=0}^{N-1} \omega_\eta^k \rho_{j+k}\Big) = 1 - \Delta x \sum_{k=0}^{N-1} \omega_\eta^k \rho_{j+k}, \tag{3.8}$$

which involves a quadrature formula to approximate the convolution term. By using the following equality

$$1 = \int_0^\eta w_\eta(x)\, dx = \sum_{k=0}^{N-1} \int_{k\Delta x}^{(k+1)\Delta x} w_\eta(x)\, dx$$

and the fact that w_η is non-increasing we obtain

$$\begin{aligned} 1 = \sum_{k=0}^{N-1} \int_{k\Delta x}^{(k+1)\Delta x} w_\eta(x)\, dx &\geq \sum_{k=0}^{N-1} w_\eta((k+1)\Delta x) \cdot \Delta x \\ &= \Delta x \cdot \sum_{k=1}^{N} w_\eta(k\Delta x) \end{aligned}$$

Thus, the above discretization choice for ω_η implies

$$\Delta x \sum_{k=0}^{N-1} w_\eta(k\Delta x) \leq 1 + w_\eta(0)\Delta x. \tag{3.9}$$

We consider the following modified Lax-Friedrichs flux adapted to (3.1):

$$F_{j+1/2}^n := g(\rho_j^n, ..., \rho_{j+N}^n) = \frac{1}{2}\rho_j^n V_j^n + \frac{1}{2}\rho_{j+1}^n V_{j+1}^n + \frac{\alpha}{2}(\rho_j^n - \rho_{j+1}^n), \tag{3.10}$$

where $\alpha \geq 1$ is the viscosity coefficient. This gives the following $N+2$ points finite volume scheme

$$\rho_j^{n+1} = H(\rho_{j-1}^n, ..., \rho_{j+N}^n), \tag{3.11}$$

where

$$\begin{aligned} H(\rho_{j-1}, ..., \rho_{j+N}) &:= \rho_j - \lambda(g(\rho_j, ..., \rho_{j+N}) - g(\rho_{j-1}, ..., \rho_{j+N-1}) \\ &= \rho_j + \frac{\lambda\alpha}{2}(\rho_{j-1} - 2\rho_j + \rho_{j+1}) + \frac{\lambda}{2}(\rho_{j-1}V_{j-1} - \rho_{j+1}V_{j+1}), \end{aligned} \tag{3.12}$$

with $\alpha = \Delta t/\Delta x$.

It is straightforward that $H(\rho, ..., \rho) = \rho$ for all $\rho \in [0, 1]$ and the numerical flux (3.10) satisfies the following assumptions:

Consistency:

$$g(\rho, ..., \rho) = \rho\Big(1 - \rho\Delta x \sum_{k=0}^{N-1} \omega_\eta^k\Big). \tag{3.13}$$

In particular, $g(\rho, ..., \rho) \to g(1 - \rho *_d \omega_\eta)$ as $\Delta x \searrow 0$ for a constant ρ.

Lipschitz continuity: There exists $\kappa > 0$ such that

$$|g(\rho_j, ..., \rho_{j+N}) - g(\rho, ..., \rho)| \leq \kappa \max_{0 \leq k \leq N} |\rho_{j+k} - \rho| \tag{3.14}$$

for $\rho, \rho_{j+k} \in [0, 1]$ and $k = 0, ..., N$. The inequality (3.9) guarantees that this is verified for $\kappa = 2 + \alpha + \omega_\eta(0)\Delta x$.

Assuming $\rho_i \in [0, 1]$ for $i = j - 1, ..., j + N$, we compute the partial derivatives of H:

$$\begin{aligned}\frac{\partial H}{\partial \rho_{j-1}} &= \frac{\lambda}{2}\Big(\alpha + V_{j-1} + \rho_{j-1}\frac{\partial V_{j-1}}{\partial \rho_{j-1}} - \rho_{j+1}\frac{\partial V_{j+1}}{\partial \rho_{j-1}}\Big) \\ &= \frac{\lambda}{2}\Big(\alpha + v\Big(\Delta x \sum_{k=0}^{N-1} \omega_\eta^k \rho_{j-1+k}\Big) + \rho_{j-1} v'\Big(\Delta x \sum_{k=0}^{N-1} \omega_\eta^k \rho_{j-1+k}\Big)\Delta x \omega_\eta^0\Big) \\ &= \frac{\lambda}{2}\Big(\alpha + 1 - \Delta x \sum_{k=0}^{N-1} \omega_\eta^k \rho_{j-1+k} - \omega_\eta^0 \rho_{j-1}\Big), \end{aligned} \tag{3.15a}$$

$$\begin{aligned}\frac{\partial H}{\partial \rho_j} &= 1 - \lambda\alpha + \frac{\lambda}{2}\Big(\rho_{j-1}\frac{\partial V_{j-1}}{\partial \rho_j} - \rho_{j+1}\frac{\partial V_{j+1}}{\partial \rho_j}\Big) \\ &= 1 - \lambda\alpha + \frac{\lambda}{2}\rho_{j-1} v'\Big(\Delta x \sum_{k=0}^{N-1} \omega_\eta^k \rho_{j-1+k}\Big)\Delta x \omega_\eta^1 \\ &= 1 - \lambda\Big(\alpha + \frac{1}{2}\Delta x \omega_\eta^1 \rho_{j-1}\Big) \geq 1 - \lambda\Big(\alpha + \Delta x \frac{\omega_\eta^0}{2}\Big), \end{aligned} \tag{3.15b}$$

$$\begin{aligned}\frac{\partial H}{\partial \rho_{j+1}} &= \frac{\lambda}{2}\Big(\alpha + \rho_{j-1}\frac{\partial V_{j-1}}{\partial \rho_{j+1}} - V_{j+1} - \rho_{j+1}\frac{\partial V_{j+1}}{\partial \rho_{j+1}}\Big) = \frac{\lambda}{2}\Big(\alpha + \rho_{j-1} v'\Big(\Delta x \sum_{k=0}^{N-1} \omega_\eta^k \rho_{j-1+k}\Big)\Delta x \omega_\eta^2 \\ &\quad - \rho_{j+1} v'\Big(\Delta x \sum_{k=0}^{N-1} \omega_\eta^k \rho_{j+1+k}\Big)\Delta x \omega_\eta^0 - v\Big(\Delta x \sum_{k=0}^{N-1} \omega_\eta^k \rho_{j+1+k}\Big)\Big) \\ &= \frac{\lambda}{2}\Big(\alpha - 1 + \Delta x \sum_{k=0}^{N-1} \omega_\eta^k \rho_{j+1+k} - \Delta x \omega_\eta^2 \rho_{j-1} + \Delta x \omega_\eta^0 \rho_{j+1}\Big), \end{aligned} \tag{3.15c}$$

$$\begin{aligned}\frac{\partial H}{\partial \rho_{j+k}} &= \frac{\lambda}{2}\Delta x\Big(\rho_{j-1}\omega_\eta^{k+1} v'\Big(\Delta x \sum_{k=0}^{N-1} \omega_\eta^k \rho_{j-1+k}\Big) - \omega_\eta^{k-1}\rho_{j+1} v'\Big(\Delta x \sum_{k=0}^{N-1} \omega_\eta^k \rho_{j+1+k}\Big)\Big), \\ &= \frac{\lambda}{2}\Delta x(\omega_\eta^{k-1}\rho_{j+1} - \omega_\eta^{k+1}\rho_{j-1}) \quad k = 2, ..., N-2 \end{aligned} \tag{3.15d}$$

$$\frac{\partial H}{\partial \rho_{j+N-1}} = -\frac{\lambda}{2}\Delta x \omega_\eta^{N-2}\rho_{j+1} v'\Big(\Delta x \sum_{k=0}^{N-1} \omega_\eta^k \rho_{j+1+k}\Big) = \frac{\lambda}{2}\Delta x \omega_\eta^{N-2}\rho_{j+1}, \tag{3.15e}$$

$$\frac{\partial H}{\partial \rho_{j+N}} = -\frac{\lambda}{2}\Delta x \omega_\eta^{N-1}\rho_{j+1} v'\Big(\Delta x \sum_{k=0}^{N-1}\omega_\eta^k \rho_{j+1+k}\Big) = \frac{\lambda}{2}\Delta x \omega_\eta^{N-1}\rho_{j+1}, \tag{3.15f}$$

Observe that (3.15e) and (3.15f) are non-negative. Moreover the CFL condition

$$\Delta t \leq \frac{2}{2\alpha + \Delta x \omega_\eta(0)}\Delta x \tag{3.16}$$

ensures the positivity of (3.15b) and the assumption

$$\alpha \geq 1 + \Delta x \omega_\eta(0) \tag{3.17}$$

guarantees the increasing monotonicity with respect to ρ_{j+1} in (3.15c), and combined with (3.9), guarantees the non-negativity of (3.15a). To obtain (3.16) and (3.17) we used the fact that $\omega_\eta^k \leq \omega_\eta(0)$ for all $k = 0, ..., N-1$, by non-increasing monotonicity of ω_η. On the other hand, the sign of (3.15d) cannot be a-priori determined. Therefore, the numerical scheme (3.10)-(3.11) is not monotone and classical convergence results do not apply.

3.2.1 Maximum principle and $\mathbf{L}^\infty$ estimates

The $\mathbf{L}^\infty$ bound is the direct consequence of a maximum principle property which is proven below by following [2].

Proposition 1. For any intial datum $\rho_j^0, j \in \mathbb{Z}$, let $\rho_m = \min_{j\in\mathbb{Z}}\{\rho_j^0\} \in [0,1]$ and $\rho_M = \max_{j\in\mathbb{Z}}\{\rho_j^0\} \in [0,1]$. Then the finite volume approximation $\rho_j^n, j \in \mathbb{Z}$ and $n \in \mathbb{N}$, constructed using scheme (3.10)-(3.11) satisfies the bounds

$$\rho_m \leq \rho_j^n \leq \rho_M$$

for all $j \in \mathbb{Z}$ and $n \in \mathbb{N}$, under the CFL condition (3.16).

The proof is a direct consequence of the following lemma.

Lemma 1. Let $0 \leq \rho_m \leq \rho_j^n \leq \rho_M \leq 1$ for all $j \in \mathbb{Z}$. Then

$$H(\rho_m, \rho_m, \rho_m, \rho_{j+2}, ..., \rho_{j+N-2}, \rho_m, \rho_m) \geq \rho_m, \tag{3.18}$$

$$H(\rho_m, \rho_m, \rho_m, \rho_{j+2}, ..., \rho_{j+N-2}, \rho_M, \rho_M) \leq \rho_M. \tag{3.19}$$

Proof. From (3.12) we get

$$\begin{aligned} H(\rho_m, \rho_m, \rho_m, \rho_{j+2}, ..., \rho_{j+N-2}, \rho_m, \rho_m) &= \rho_m + \frac{\Delta t}{2}\rho_m(V_{j-1} - V_{j+1}) \\ &= \rho_m + \frac{\Delta t}{2}\rho_m\Big(v\Big(\Delta x \sum_{k=0}^{N-1}\omega_\eta^k \rho_{j-1+k}\Big) - v\Big(\Delta x \sum_{k=0}^{N-1}\omega_\eta^k \rho_{j+1+k}\Big)\Big) \end{aligned}$$

From the mean value theorem we obtain

$$v\Big(\Delta x\sum_{k=0}^{N-1}\omega_\eta^k\rho_{j-1+k}\Big)-v\Big(\Delta x\sum_{k=0}^{N-1}\omega_\eta^k\rho_{j+1+k}\Big)=v'(\xi)\left[\Delta x\sum_{k=0}^{N-1}\omega_\eta^k(\rho_{j-1+k}-\rho_{j+1+k})\right]\geq 0,$$

for some ξ between $\Delta x\sum_{k=0}^{N-1}\omega_\eta^k\rho_{j-1+k}$ and $\Delta x\sum_{k=0}^{N-1}\omega_\eta^k\rho_{j+1+k}$. Indeed, we observe that

$$\sum_{k=0}^{N-1}\omega_\eta^k(\rho_{j+1+k}-\rho_{j-1+k})=\rho_m[\omega_\eta^{N-2}+\omega_\eta^{N-1}-\omega_\eta^0-\omega_\eta^1]+\sum_{k=1}^{N-2}\rho_{j+k}[\omega_\eta^{k-1}-\omega_\eta^{k+1}]$$
$$\geq\rho_m[\omega_\eta^{N-2}+\omega_\eta^{N-1}-\omega_\eta^0-\omega_\eta^1]+\rho_m\sum_{k=1}^{N-2}[\omega_\eta^{k-1}-\omega_\eta^{k+1}]=\rho_m\left\{\sum_{k=1}^{N}\omega_\eta^{k-1}-\sum_{k=-1}^{N-2}\omega_\eta^{k+1}\right\}=0,$$

where the inequality is due to the non-increasing monotonicity of ω_η. Inequality (3.19) can be recovered in a similar way.

Proof of Proposition 1. We apply the mean value theorem between the points $R_j^n=(\rho_{j-1}^n,...,\rho_{j+N}^n)$ and $R_m^n=(\rho_m,\rho_m,\rho_m,\rho_{j+2}^n,...,\rho_{j+N-2}^n,\rho_m,\rho_m)$. By (3.18)

$$\rho_j^{n+1}=H(R_j^n)=H(R_m^n)+\langle\nabla H(R_\xi),R_j^n-R_m^n\rangle\geq\rho_m+\langle\nabla H(R_\xi),R_j^n-R_m^n\rangle,\quad(3.20)$$

for $R_\xi=(1-\xi)R_m^n+\xi R_j^n$, for some $\xi\in[0,1]$.

It is now enough to observe that

$$\frac{\partial H}{\partial\rho_{j+k}}(R_\xi)(R_j^n-R_m^n)_k=0,\quad k=2,...,N-2,$$

since $(R_j^n-R_m^n)_k=0$ for $k=2,...,N-2$. Therefore, under the assumptions (3.16) and (3.17), we can conclude that $\langle\nabla H(R_\xi),R_j^n-R_m^n\rangle\geq 0$ and therefore by (3.20) we have proved that

$$\rho_j^{n+1}\geq\rho_m$$

. The upper bound $\rho_j^{n+1}\leq\rho_M$ can be recovered similarly by considering

$$R_M^n=(\rho_M,\rho_M,\rho_M,\rho_{j+2}^n,...,\rho_{j+N-2}^n,\rho_M,\rho_M)$$

in place of R_m^n and using (3.19).

3.2.2 BV estimates

Accurate estimates show that the approximate solutions constructed using the given numerical scheme have bounded total variation and preserve monotonicity.

Proposition 2: Let $\rho_0 \in BV(\mathbb{R};[0,1]$, and let $\rho_{\Delta x}$ be given by (3.11)-(3.12). If $\alpha \geq 1+2\Delta x w_\eta(0)$ and the CFL condition $\Delta t \leq 2\Delta x/(2\alpha+3\Delta x w_\eta(0))$ holds, then for every $T>0$ the following discrete space BV estimate is satisfied

$$TV(\rho_{\Delta x}(T,\cdot)) \leq C(w_\eta(0),\rho_0,T) := e^{2w_\eta(0)T}TV(\rho_0) \tag{3.21}$$

In particular, the numerical scheme (3.11)-(3.12) is monotonicity preserving.

Proof. Writing scheme (3.11)-(3.12) as:

$$\begin{aligned}
\rho_j^{n+1} = \rho_j^n &- \frac{\lambda}{2}\Big(\alpha+1-\Delta x\sum_{k=0}^{N-1} w_\eta^k\rho_{j+k+1}^n - \Delta x w_\eta^0\rho_{j-1}^n\Big)\Delta_{j-1/2}^n \\
&+ \frac{\lambda}{2}\Big(\alpha-1+\Delta x\sum_{k=0}^{N-1} w_\eta^k\rho_{j+k+1}^n + \Delta x(w_\eta^0+w_\eta^1)\rho_{j-1}^n\Big)\Delta_{j+1/2}^n \\
&+ \frac{\lambda}{2}\rho_{j-1}^n\Delta x\sum_{k=2}^{N-1}(w_\eta^{k-1}+w_\eta^k)\Delta_{j+k-1/2}^n + \frac{\lambda}{2}\Delta x w_\eta^{N-1}\rho_{j-1}^n\Delta_{j+N-1/2}^n,
\end{aligned}$$

where $\Delta_{j+k-1/2}^n = \rho_{j+k}^n - \rho_{j+k-1}^n$ for $k=0,...,N$. Similarly,

$$\begin{aligned}
\rho_{j+1}^{n+1} = \rho_{j+1}^n &- \frac{\lambda}{2}\Big(\alpha+1-\Delta x\sum_{k=0}^{N-1} w_\eta^k\rho_{j+k+2}^n - \Delta x w_\eta^0\rho_j^n\Big)\Delta_{j+1/2}^n \\
&+ \frac{\lambda}{2}\Big(\alpha-1+\Delta x\sum_{k=0}^{N-1} w_\eta^k\rho_{j+k+2}^n + \Delta x(w_\eta^0+w_\eta^1)\rho_j^n\Big)\Delta_{j+3/2}^n \\
&+ \frac{\lambda}{2}\rho_j^n\Delta x\sum_{k=2}^{N-1}(w_\eta^{k-1}+w_\eta^k)\Delta_{j+k+1/2}^n + \frac{\lambda}{2}\Delta x w_\eta^{N-1}\rho_j^n\Delta_{j+N+1/2}^n,
\end{aligned}$$

Therefore, computing the difference yields:

$$\begin{aligned}
\Delta_{j+1/2}^{n+1} = &\frac{\lambda}{2}\Big(\alpha+1-\Delta x\sum_{k=0}^{N-1} w_\eta^k\rho_{j+k+1}^n - \Delta x w_\eta^0\rho_{j-1}^n\Big)\Delta_{j-1/2}^n \\
&+ \Big[1-\frac{\lambda}{2}\Big(2\alpha-\Delta x w_\eta^0\rho_j^n + \Delta x(w_\eta^0+w_\eta^1)\rho_{j-1}^n - \Delta x\sum_{k=0}^{N-1} w_\eta^k\Delta_{j+k+3/2}\Big)\Big]\Delta_{j+1/2}^n \\
&+ \frac{\lambda}{2}\Big[\Big(\alpha-1+\Delta x(w_\eta^0+w_\eta^1)\rho_j^n - \Delta x(w_\eta^1+w_\eta^2)\rho_{j-1}^n + \Delta x\sum_{k=0}^{N-1} w_\eta^k\Delta_{j+k+2}\Big)\Big]\Delta_{j+3/2}^n \\
&+ \frac{\lambda}{2}\Delta x\sum_{k=2}^{N-2}\Big[(w_\eta^{k-1}+w_\eta^k)\rho_j^n - (w_\eta^k+w_\eta^{k+1})\rho_{j-1}^n\Big]\Delta_{j+k+1/2}^n \\
&+ \frac{\lambda}{2}\Delta x\Big[(w_\eta^{N-2}+w_\eta^{N-1})\rho_j^n - w_\eta^{N-1}\rho_{j-1}^n\Big]\Delta_{j+N-1/2}^n + \frac{\lambda}{2}\Delta x w_\eta^{N-1}\rho_j^n\Delta_{j+N+1/2}^n.
\end{aligned}$$

Adding and subtracting $(w_\eta^k + w_\eta^{k+1})\rho_j^n$ to the fourth term of right hand side of the above equality, and observing that

$$\Big[(w_\eta^{N-2} + w_\eta^{N-1})\rho_j^n - w_\eta^{N-1}\rho_{j-1}^n\Big]\Delta_{j+N-1/2}^n = \Big[w_\eta^{N-2}\rho_j^n + w_\eta^{N-1}\Delta_{j-1/2}^n\Big]\Delta_{j+N-1/2}^n,$$

we obtain

$$\begin{aligned}
\Delta_{j+1/2}^{n+1} = {} & \frac{\lambda}{2}\Big(\alpha + 1 - \Delta x w_\eta^0(\rho_{j-1}^n + \rho_{j+1}^n) - \Delta x(w_\eta^1 + w_\eta^2)\rho_{j+2}^n - \Delta x\sum_{k=2}^{N-2} w_\eta^{k+1}\rho_{j+k}^n\Big)\Delta_{j-1/2}^n \\
& + \Big[1 - \frac{\lambda}{2}\Big(2\alpha - \Delta x w_\eta^0\rho_j^n + \Delta x(w_\eta^0 + w_\eta^1)\rho_{j-1}^n - \Delta x\sum_{k=0}^{N-1} w_\eta^k\Delta_{j+k+3/2}\Big)\Big]\Delta_{j+1/2}^n \\
& + \frac{\lambda}{2}\Big(\alpha - 1 + \Delta x(w_\eta^0 + w_\eta^1)\rho_j^n - \Delta x(w_\eta^1 + w_\eta^2)\rho_{j-1}^n + \Delta x\sum_{k=0}^{N-1} w_\eta^k\rho_{j+k+2}\Big)\Delta_{j+3/2}^n \\
& + \frac{\lambda}{2}\rho_j^n\Delta x\sum_{k=2}^{N-2}(w_\eta^{k-1} - w_\eta^{k+1})\Delta_{j+k+1/2}^n \\
& + \frac{\lambda}{2}\Delta x w_\eta^{N-2}\rho_j^n\Delta_{j+N-1/2}^n + \frac{\lambda}{2}\Delta x w_\eta^{N-1}\rho_j^n\Delta_{j+N+1/2}^n
\end{aligned}$$

It's important to note that the first coefficient in the summation is non-negative for Δx sufficiently small such that $\alpha \geq 2w_\eta(0)\Delta x$, since

$$\begin{aligned}
& \Delta x w_\eta^0(\rho_{j-1}^n + \rho_{j+1}^n) - \Delta x(w_\eta^1 + w_\eta^2)\rho_{j+2}^n - \Delta x\sum_{k=2}^{N-2} w_\eta^{k+1}\rho_{j+k}^n \\
& \leq \Delta x w_\eta^0 + \Delta x\sum_{k=0}^{N-1} w_\eta^k \leq 1 + 2w_\eta(0)\Delta x
\end{aligned}$$

by (3.9). A slightly stronger CFL assumption

$$\Delta t \leq \frac{2}{2\alpha + 3\Delta x w_\eta(0)}\Delta x$$

makes the second coefficient in the summation non-negative and the third term is non-negative if $\alpha \geq 1 + 2\Delta x w_\eta(0)$. Thus, all the coefficients in the above expressions are non-negative and the formula given above guarantees that the scheme (3.11)-(3.12) is monotonicity preserving. Next, we take the absolute values in the above expression and

sum them over $j \in \mathbb{Z}$ and this process gives

$$
\begin{aligned}
&\Rightarrow \sum_j \left|\Delta_{j+1/2}^{n+1}\right| \\
&= \sum_j \frac{\lambda}{2}\Big(\alpha + 1 - \Delta x w_\eta^0(\rho_{j-1}^n + \rho_{j+1}^n) - \Delta x(w_\eta^1 + w_\eta^2)\rho_{j+2}^n - \Delta x \sum_{k=2}^{N-2} w_\eta^{k+1}\rho_{j+k}^n\Big)\left|\Delta_{j-1/2}^n\right| \\
&+ \sum_j \Big[1 - \frac{\lambda}{2}\Big(2\alpha - \Delta x w_\eta^0\rho_j^n + \Delta x(w_\eta^0 + w_\eta^1)\rho_{j-1}^n - \Delta x \sum_{k=0}^{N-1} w_\eta^k \Delta_{j+k+3/2}\Big)\Big]\left|\Delta_{j+1/2}^n\right| \\
&+ \sum_j \frac{\lambda}{2}\Big(\alpha - 1 + \Delta x(w_\eta^0 + w_\eta^1)\rho_j^n - \Delta x(w_\eta^1 + w_\eta^2)\rho_{j-1}^n + \Delta x \sum_{k=0}^{N-1} w_\eta^k \rho_{j+k+2}\Big)\left|\Delta_{j+3/2}^n\right| \\
&+ \sum_j \frac{\lambda}{2}\rho_j^n \Delta x \sum_{k=2}^{N-2}(w_\eta^{k-1} - w_\eta^{k+1})\left|\Delta_{j+k+1/2}^n\right| + \sum_j \frac{\lambda}{2}\Delta x w_\eta^{N-2}\rho_j^n\left|\Delta_{j+N-1/2}^n\right| \\
&+ \sum_j \frac{\lambda}{2}\Delta x w_\eta^{N-1}\rho_j^n\left|\Delta_{j+N+1/2}^n\right|
\end{aligned}
$$

Rearranging the terms gives

$$
\begin{aligned}
\sum_j \left|\Delta_{j+1/2}^{n+1}\right| &= \sum_j \left|\Delta_{j+1/2}^n\right|\Big[1 + \frac{\Delta t}{2}\Big(\sum_{k=2}^{N-2}(w_\eta^{k-1} - w_\eta^{k+1})\rho_{j+k+1}^n - (w_\eta^1 + w_\eta^2)\rho_{j-2}^n \\
&\quad + \sum_{k=2}^{N-2}(w_\eta^{k-1} - w_\eta^{k+1})\rho_{j-k}^n - (w_\eta^1 + w_\eta^2)\rho_{j+3}^n + w_\eta^{N-2})\rho_{j+N}^n \\
&\quad + w_\eta^{N-1}\rho_{j+N+1}^n + w_\eta^{N-2}\rho_{j-N-1}^n + w_\eta^{N-1})\rho_{j-N}^n\Big)\Big] \\
&\le \Big[1 + \frac{\Delta t}{2}\Big(\sum_{k=2}^{N-2}(w_\eta^{k-1} - w_\eta^{k+1}) + 2w_\eta^{N-2} + 2w_\eta^{N-1}\Big)\Big]\sum_j \left|\Delta_{j+1/2}^n\right| \\
&\le (1 + 2w_{\eta(0)}\Delta t)\sum_j \left|\Delta_{j+1/2}^n\right|
\end{aligned}
$$

Hence we get the following estimate for the total variation

$$TV(\rho_{\Delta x}(T,\cdot)) \le (1 + 2w_\eta(0)\Delta t)^{T/\Delta t} TV(\rho_{\Delta x}(0,\cdot)) \le e^{2w_\eta(0)T} TV(\rho_0).$$

Following [2], we derive the following space-time BV estimate;

Corollary 1. Let $\rho_0 \in BV(\mathbb{R};[0,1])$, and $\rho_{\Delta x}$ be given by (3.11)-(3.12). If $\alpha \ge 1 + 2\Delta x w_\eta(0)$ and $\Delta t \le 2\Delta x/(2\alpha + 3\Delta x w_\eta(0))$, then for every $T > 0$ there exists $\bar{C} = \bar{C}(w_\eta, \rho_0, T, \alpha)$ such that

$$TV(\rho_{\Delta x}; [0,T] \times R) \le \bar{C} \tag{3.22}$$

3.2.3 Discrete entropy inequalities

We derive a discrete entropy inequality for the approximate solution generated by the scheme (3.11)-(3.12).

$$G_{j+1/2}(u,v) = \frac{1}{2}uV_j^n + \frac{1}{2}vV_{j+1}^n + \frac{\alpha}{2}(u-v),$$
$$F_{j+1/2}^{\kappa}(u,v) = G_{j+1/2}(u\wedge\kappa, v\wedge\kappa) - G_{j+1/2}(u\vee\kappa, v\vee\kappa)$$

where $a\wedge b = \max(a,b)$ and $a\vee b = \min(a,b)$.

Proposition 3. Let ρ_j^n, $j\in\mathbb{Z}$, $n\in\mathbb{N}$, be given by (3.10)-(3.11). Then, if $\alpha\geq 1$ and the CFL condition (3.16) holds, for all $j\in\mathbb{Z}$, $n\in\mathbb{N}$ we have

$$|\rho_j^{n+1}-\kappa| - |\rho_j^n-\kappa| + \lambda\Big(F_{j+1/2}^{\kappa}(\rho_j^n,\rho_{j+1}^n) - F_{j-1/2}^{\kappa}(\rho_{j-1}^n,\rho_j^n)\Big) + \frac{\lambda}{2}sgn(\rho_j^{n+1}-\kappa)\kappa(V_{j+1}^n - V_{j-1}^n) \leq 0 \tag{3.23}$$

for all $\kappa\in\mathbb{R}$.

Proof. With

$$\bar{H}_j(u,v,z) = v - \lambda(G_{j+1/2}(v,z) - G_{j-1/2}(u,v)),$$

from (3.16) we have that the function $\bar{H}_j$ is monotone non-decreasing in its first variable, montone non-decreasing in its second variable for $\alpha\lambda\leq 1$ and (3.17) guarantees that for $\alpha\geq 1$ it is monotone non-decreasing in its third variable. Moreover, we have the identity

$$\bar{H}_j(\rho_{j-1}^n\wedge\kappa, \rho_j^n\wedge\kappa, \rho_{j+1}^n\wedge\kappa) - \bar{H}_j(\rho_{j-1}^n\vee\kappa, \rho_j^n\vee\kappa, \rho_{j+1}^n\vee\kappa)$$
$$= |\rho_j^n-\kappa| - \lambda\Big(F_{j+1/2}^{\kappa}(\rho_j^n,\rho_{j+1}^n) - F_{j-1/2}^{\kappa}(\rho_{j-1}^n,\rho_j^n)\Big).$$

By monotonicity,

$$
\begin{aligned}
&\Rightarrow \bar{H}_j(\rho_{j-1}^n \wedge \kappa, \rho_j^n \wedge \kappa, \rho_{j+1}^n \wedge \kappa) - \bar{H}_j(\rho_{j-1}^n \vee \kappa, \rho_j^n \vee \kappa, \rho_{j+1}^n \vee \kappa) \\
&= \bar{H}_j(\rho_{j-1}^n, \rho_j^n, \rho_{j+1}^n) \wedge \bar{H}_j(\kappa,\kappa,\kappa) - \bar{H}_j(\rho_{j-1}^n, \rho_j^n, \rho_{j+1}^n) \vee \bar{H}_j(\kappa,\kappa,\kappa) \\
&= \Big|\bar{H}_j(\rho_{j-1}^n, \rho_j^n, \rho_{j+1}^n) - \bar{H}_j(\kappa,\kappa,\kappa)\Big| \\
&= sgn\Big(\bar{H}_j(\rho_{j-1}^n, \rho_j^n, \rho_{j+1}^n) - \bar{H}_j(\kappa,\kappa,\kappa)\Big) \times \Big(\bar{H}_j(\rho_{j-1}^n, \rho_j^n, \rho_{j+1}^n) - \bar{H}_j(\kappa,\kappa,\kappa)\Big) \\
&= sgn\Big(\bar{H}_j(\rho_{j-1}^n, \rho_j^n, \rho_{j+1}^n) - \kappa + \frac{\lambda}{2}\kappa(V_{j+1}^n - V_{j-1}^n)\Big) \\
&\times \Big(\bar{H}_j(\rho_{j-1}^n, \rho_j^n, \rho_{j+1}^n) - \kappa + \frac{\lambda}{2}\kappa(V_{j+1}^n - V_{j-1}^n)\Big) \\
&\geq sgn\Big(\bar{H}_j(\rho_{j-1}^n, \rho_j^n, \rho_{j+1}^n) - \kappa\Big) \times \Big(\bar{H}_j(\rho_{j-1}^n, \rho_j^n, \rho_{j+1}^n) - \kappa + \frac{\lambda}{2}\kappa(V_{j+1}^n - V_{j-1}^n)\Big) \\
&= \Big|\bar{H}_j(\rho_{j-1}^n, \rho_j^n, \rho_{j+1}^n) - \kappa\Big| + \frac{\lambda}{2} sgn\Big(\bar{H}_j(\rho_{j-1}^n, \rho_j^n, \rho_{j+1}^n) - \kappa\Big)\kappa(V_{j+1}^n - V_{j-1}^n) \\
&= \Big|\rho_j^{n+1} - \kappa\Big| + \frac{\lambda}{2} sgn(\rho_j^{n+1} - \kappa)\kappa(V_{j+1}^n - V_{j-1}^n)
\end{aligned}
$$

from the definition of (3.11)-(3.12), we have (3.23).

3.2.4 $\mathbf{L^1}$ stability estimates

Since Kružkov theory cannot be applied here due to lack of regularity of the convolution kernel ω_η, we prove the explicit $\mathbf{L^1}$ estimates that guarantees the stability of the scheme (3.11)-(3.12).

Proposition 4. Let $\rho_0,\ \bar{\rho}_0 \in BV(\mathbb{R};[0,1])$ be two initial data, and denoted by $\rho_{\Delta x}$, $\rho_{\bar{\Delta} x}$ the corresponding approximate solutoins constructed applying the modified Lax-Friedrichs scheme (3.11)- (3.12):

$$\rho_j^{n+1} = \rho_j^n + \frac{\lambda\alpha}{2}(\rho_{j-1}^n - 2\rho_j^n + \rho_{j+1}^n) + \frac{\lambda}{2}(\rho_{j-1}^n V_{j-1}^n - \rho_{j+1} V_{j+1}^n), \tag{3.24}$$

$$\bar{\rho}_j^{n+1} = \bar{\rho}_j^n + \frac{\lambda\alpha}{2}(\bar{\rho}_{j-1}^n - 2\bar{\rho}_j^n + \bar{\rho}_{j+1}^n) + \frac{\lambda}{2}(\bar{\rho}_{j-1}^n \bar{V}_{j-1}^n - \bar{\rho}_{j+1} \bar{V}_{j+1}^n), \tag{3.25}$$

where we have set $V_j^n = 1 - \Delta x \sum_{k=0}^{N-1} w_\eta^k \rho_{j+k}^n$ and $\bar{V}_j^n = 1 - \Delta x \sum_{k=0}^{N-1} w_\eta^k \bar{\rho}_{j+k}^n$. Then under the assumptions (3.16), (3.17) the following estimate holds:

$$||\rho_{\Delta x}(T,\cdot) - \bar{\rho}_{\Delta x}(T,\cdot)||_{\mathbf{L^1}} \leq K(w_\eta, \rho_0, \bar{\rho}_0, T)||\rho_0 - \bar{\rho}_0||_{\mathbf{L^1}} \tag{3.26}$$

with $K(w_\eta, \rho_0, \bar{\rho}_0, T) := \exp(T w_\eta(0)(1 + 0.5\min\{C(w_\eta, \rho_0, T), C(w_\eta, \bar{\rho}_0, T)\}))$.

Proof. We subtract (3.25) from (3.24) which gives:

$$\begin{aligned}
\rho_j^{n+1} - \bar{\rho}_j^{n+1} &= (1-\lambda\alpha)(\rho_j^n - \bar{\rho}_j^n) + \frac{\lambda\alpha}{2}(\rho_{j-1}^n - \bar{\rho}_{j-1}^n) \\
&+ \frac{\lambda\alpha}{2}(\rho_{j+1}^n - \bar{\rho}_{j+1}^n) + \frac{\lambda}{2}(\rho_{j-1}^n(V_{j-1}^n - \bar{V}_{j-1}^n) + (\rho_{j-1}^n - \bar{\rho}_{j-1}^n)\bar{V}_{j-1}^n) \\
&- \frac{\lambda}{2}((\rho_{j+1}^n - \bar{\rho}_{j+1}^n)\bar{V}_{j+1}^n + (\rho_{j+1}^n(V_{j+1}^n - \bar{V}_{j+1}^n)) \\
&= \Big(1 - \lambda\alpha - \frac{\lambda}{2}\Delta x w_\eta^1 \rho_{j-1}^n\Big)(\rho_j^n - \bar{\rho}_j^n) + \frac{\lambda}{2}(\alpha + \bar{V}_{j-1}^n - \Delta x w_\eta^0 \rho_{j-1}^n)(\rho_{j-1}^n - \bar{\rho}_{j-1}^n) \\
&+ \frac{\lambda}{2}(\alpha - \bar{V}_{j+1}^n + \Delta x w_\eta^0 \rho_{j+1}^n - \Delta x w_\eta^2 \rho_{j-1}^n)(\rho_{j+1}^n - \bar{\rho}_{j+1}^n) \\
&+ \frac{\lambda}{2}\Delta x \sum_{k=2}^{N-2}(w_\eta^{k-1}\rho_{j+1}^n - w_\eta^{k+1}\rho_{j-1}^n)(\rho_{j+k}^n - \bar{\rho}_{j+k}^n) \\
&+ \frac{\lambda}{2}\Delta x w_\eta^{N-2}\rho_{j+1}^n(\rho_{j+N-1}^n - \bar{\rho}_{j+N-1}^n) + \frac{\lambda}{2}\Delta x w_\eta^{N-1}\rho_{j+1}^n(\rho_{j+N}^n - \bar{\rho}_{j+N}^n).
\end{aligned}$$

A close observation shows that from (3.16) the coefficient of the first term is positive and from (3.17) we have the coefficients of second and third terms positive. Therefore, we take the absolute values in the above equality and get

$$\begin{aligned}
|\rho_j^{n+1} - \bar{\rho}_j^{n+1}| &\le \Big(1 - \lambda\alpha - \frac{\lambda}{2}\Delta x w_\eta^1 \rho_{j-1}^n\Big)|\rho_j^n - \bar{\rho}_j^n| \\
&+ \frac{\lambda}{2}(\alpha + \bar{V}_{j-1}^n - \Delta x w_\eta^0 \rho_{j-1}^n)|\rho_{j-1}^n - \bar{\rho}_{j-1}^n| \\
&+ \frac{\lambda}{2}(\alpha - \bar{V}_{j+1}^n + \Delta x w_\eta^0 \rho_{j+1}^n - \Delta x w_\eta^2 \rho_{j-1}^n)|\rho_{j+1}^n - \bar{\rho}_{j+1}^n| \\
&+ \frac{\lambda}{2}\Delta x \sum_{k=2}^{N-2}|w_\eta^{k-1}\rho_{j+1}^n - w_\eta^{k+1}\rho_{j-1}^n||\rho_{j+k}^n - \bar{\rho}_{j+k}^n| \\
&+ \frac{\lambda}{2}\Delta x w_\eta^{N-2}\rho_{j+1}^n|\rho_{j+N-1}^n - \bar{\rho}_{j+N-1}^n| + \frac{\lambda}{2}\Delta x w_\eta^{N-1}\rho_{j+1}^n|\rho_{j+N}^n - \bar{\rho}_{j+N}^n|.
\end{aligned}$$

Next, we sum it over $j \in \mathbb{Z}$, rearrange the indexes and by monotonicity of w_η and using the triangular inequality

$$|w_\eta^{k-1}\rho_{j+1}^n - w_\eta^{k+1}\rho_{j-1}^n \le (w_\eta^{k-1} - w_\eta^{k+1})\rho_{j+1}^n + w_\eta^{k+1}|\rho_{j+1}^n - \rho_{j-1}^n|$$

we have

$$\begin{aligned}
\sum_j |\rho_j^{n+1} - \bar{\rho}_j^{n+1}| \le \Big[1 + \frac{\Delta t}{2}\Big(\sum_{k=2}^{N-2}(w_\eta^{k-1} - w_\eta^{k+1} + w_\eta^{N-2} + w_\eta^{N-1})\Big) \\
+ \frac{\Delta t}{2}\sum_{k=2}^{N-2} w_\eta^{k+1}|\rho_{j-k+1}^n - \rho_{j-k-1}^n|\Big]\sum_j |\rho_j^n - \bar{\rho}_j^n|.
\end{aligned}$$

Therefore,

$$\|\rho_{\Delta x}(T,\cdot)-\bar{\rho}_{\Delta x}(T,\cdot)\|_{\mathbf{L^1}} \leq \Big(1+\Delta t\frac{2+TV(\rho_{\Delta x})}{2}w_\eta(0)\Big)^{T/\Delta t}\|\rho_0-\bar{\rho}_0\|_{\mathbf{L^1}}$$

which gives us the estimate (3.26).

Proof of Theorem 1. To show the convergence of scheme (3.11)-(3.12) to a weak solution of 3.1, we apply the classical procedure of Lax-Wendroff theorem following [2]. Thanks to **Proposition 1** and **Corollary 1**, we can apply Helly's theorem, stating that there exists a subsequence, still denoted by $\rho_{\Delta x}$, that converges to some $\rho \in (\mathbf{L^1}\cap\mathbf{L^\infty}\cap BV)(\mathbb{R}^+\times\mathbb{R};[0,1])$ in the $\mathbf{L^1}_{loc}$-norm.
Let $\phi\in C_c^1(\mathbb{R}^2)$ and then multiply (3.11) by $\phi(t^n,x_j)$ and sum it over $j\in\mathbb{Z}$ and $n\in\mathbb{N}$ and this process yields

$$\sum_n\sum_j \phi(t^n,x_j)(\rho_j^{n+1}-\rho_j^n) = -\lambda\sum_n\sum_j \phi(t^n,x_j)(g(\rho_j^n,...,\rho_{j+N}^n)-g(\rho_{j-1}^n,...,\rho_{j+N-1}^n))$$

Summation by parts gives

$$\begin{aligned}\sum_j \phi(0,x_j)\rho_j^0 &+ \sum_n\sum_j(\phi(t^n,x_j)-\phi(t^{n-1},x_j))\rho_j^n\\ &+\lambda\sum_n\sum_j(\phi(t^n,x_{j+1})-\phi(t^n,x_j))g(\rho_j^n,...,\rho_{j+N}^n)=0\end{aligned}\tag{3.27}$$

Next we multiply the above equation by Δx

$$\begin{aligned}\Delta x\sum_j \phi(0,x_j)\rho_j^0 &+ \Delta x\Delta t\sum_n\sum_j\frac{\phi(t^n,x_j)-\phi(t^{n-1},x_j)}{\Delta t}\rho_j^n\\ &+\Delta x\Delta t\sum_n\sum_j\frac{\phi(t^n,x_{j+1})-\phi(t^n,x_j)}{\Delta x}g(\rho_j^n,...,\rho_{j+N}^n)=0.\end{aligned}\tag{3.28}$$

By strong $\mathbf{L^1_{loc}}$ convergence of $\rho_{\Delta x}\longrightarrow\rho$, it is easy to see that the first two terms in (3.28) converge to

$$\int_{-\infty}^{+\infty}\rho_0(x)\phi(0,x)dx+\int_0^{+\inf}\int_{-\infty}^{+\infty}\rho(t,x)\phi_t(t,x)dxdt$$

as $\Delta \searrow 0$. Concerning the last term, since $\rho_j^n \in [0.1]$ we observe that

$$\begin{aligned}
|g(\rho_j^n, ..., \rho_{j+N}^n) - \rho_j^n V_j^n| &\leq \frac{\alpha}{2}|\rho_{j+1}^n - \rho_j^n| + \frac{1}{2}|\rho_{j+1}^n V_{j+1}^n - \rho_j^n V_j^n| \\
&\leq \frac{\alpha}{2}|\rho_{j+1}^n - \rho_j^n| + \frac{1}{2}|(\rho_{j+1}^n - \rho_j^n)V_{j+1}^n + \rho_j^n(V_{j+1}^n - V_j^n)| \\
&\leq \frac{1+\alpha}{2}|\rho_{j+1}^n - \rho_j^n| + \frac{1}{2}\rho_j^n \Delta x \sum_{k=0}^{N-1} w_\eta^k |\rho_{j+k+1}^n - \rho_{j+k}^n| \\
&\leq \frac{1+\alpha}{2}|\rho_{j+1}^n - \rho_j^n| + \frac{1}{2} w_\eta(0) TV(\rho_{\Delta x}(t^n, \cdot))\Delta x \\
&\leq \frac{1+\alpha}{2}|\rho_{j+1}^n - \rho_j^n| + C'(w_\eta, \rho_0, T)\Delta x, \qquad (3.29)
\end{aligned}$$

where $C'(w_\eta, \rho_0, T) = w_\eta(0)C(w_\eta, \rho_0, T)/2$ for $T \geq t^n$. Therefore, writing the last term in (3.28) as

$$\begin{aligned}
&\Rightarrow \Delta x \Delta t \sum_n \sum_j \frac{\phi(t^n, x_{j+1}) - \phi(t^n, x_j)}{\Delta x} g(\rho_j^n, ..., \rho_{j+N}^n) \\
&= \Delta x \Delta t \sum_n \sum_j \frac{\phi(t^n, x_{j+1}) - \phi(t^n, x_j)}{\Delta x} \rho_j^n V_j^n \\
&+ \Delta x \Delta t \sum_n \sum_j \frac{\phi(t^n, x_{j+1}) - \phi(t^n, x_j)}{\Delta x} (g(\rho_j^n, ..., \rho_{j+N}^n) - \rho_j^n V_j^n)
\end{aligned}$$

By consistency, the first term in the above expression converges to

$$\int_0^\infty \int_{-\infty}^{+\infty} \rho(t,x) v(\rho *_d w_\eta(t,x) \phi_x(t,x) dx dt,$$

and the second term can be bounded using (3.29) in the following way:

Set $T > 0$ and $R > 0$ such that $\phi(t,x) = 0$ for $t > T$ and $|x| > R$, and let $n_T \in \mathbb{N}$ and $j_0, j_1 \in \mathbb{Z}$ such that $T \in]n_T \Delta t, (n_T+1)\Delta t]$, $-R \in]x_{j_0 - 1/2}, x_{j_0+1/2}]$ and $R \in]x_{j_1-1/2}, x_{j_1+1/2}]$. Then,

$$\begin{aligned}
&\Rightarrow \Delta x \Delta t \sum_n \sum_j \frac{\phi(t^n, x_{j+1}) - \phi(t^n, x_j)}{\Delta x} (g(\rho_j^n, ..., \rho_{j+N}^n) - \rho_j^n V_j^n) \\
&\leq \Delta x \Delta t \|\phi_x\|_\infty \sum_{n=0}^{n_T} \sum_{j=j_0}^{j_1} \left(\frac{1+\alpha}{2} |\rho_{j+1}^n - \rho_j^n + C'(w_\eta, \rho_0, T)\Delta x \right) \\
&= \frac{1+\alpha}{2} \Delta x \Delta t \|\phi_x\|_\infty \sum_{n=0}^{n_T} \sum_{j=j_0}^{j_1} |\rho_{j+1}^n - \rho_j^n| + \|\phi_x\|_\infty C'(w_\eta, \rho_0, T) 2RT\Delta x \\
&\leq \frac{1+\alpha}{2} \|\phi_x\|_\infty \int_0^T \int_{-R}^R |\rho_{\Delta x}(t, x+\Delta x) - \rho_{\Delta x}(t,x)| dx dt + \|\phi_x\|_\infty C'(w_\eta, \rho_0, T) 2RT\Delta x \\
&\leq \frac{1+\alpha}{2} \|\phi_x\|_\infty C(w_\eta, \rho_0, T)\Delta x + \|\phi_x\|_\infty C'(w_\eta, \rho_0, T) 2RT\Delta x, \qquad (3.30)
\end{aligned}$$

which tends to zero when $\Delta x \searrow 0$. For the entropy condition, we carry out the same steps as above to show that (3.23) converges to (3.6). We multiply (3.23) by $\Delta x \phi(t^n, x_j) \geq 0$ and then summing by parts yields

$$
\begin{aligned}
0 \leq \Delta x \sum_j \phi(0, x_j)|\rho_j^0 - \kappa| + \Delta x \Delta t \sum_n \sum_j \frac{\phi(t^n, x_j) - \phi(t^{n-1}, x_j)}{\Delta t}|\rho_j^n - \kappa| \\
+ \Delta x \Delta t \sum_n \sum_j \frac{\phi(t^n, x_{j+1}) - \phi(t^n, x_j)}{\Delta x} F^{\kappa}_{j+1/2}(\rho_j^n, \rho_{j+1}^n) \\
- \Delta x \Delta t \sum_n \sum_j \operatorname{sgn}(\rho_j^{n+1} - \kappa)\kappa \frac{V_{j+1}^n - V_{j-1}^n}{2\Delta x}\phi(t^n, x_j).
\end{aligned}
$$

We follow the same steps as above and observe that as $\Delta x \searrow 0$ the first three terms in the sum converge to

$$
\begin{aligned}
\int_0^{+\infty} \int_{-\infty}^{+\infty} (|\rho(t,x) - k|\phi_t + |\rho(t,x) - k| v(\rho *_d w_\eta(t,x))\phi_x) dx dt \\
+ \int_{-\infty}^{+\infty} |\rho_0(x) - \kappa|\phi(0,x) dx.
\end{aligned}
$$

Writing third term as

$$
\begin{aligned}
&\sum_n \sum_j \operatorname{sgn}(\rho_j^{n+1} - \kappa)\kappa \frac{V_{j+1}^n - V_{j-1}^n}{2\Delta x}\phi(t^n, x_j). \\
&\quad = (\operatorname{sgn}(\rho_j^{n+1} - \kappa) - \operatorname{sgn}(\rho_j^n - \kappa))\kappa \frac{V_{j+1}^n - V_{j-1}^n}{2\Delta x}\phi(t^n, x_j). \\
&\qquad + \operatorname{sgn}(\rho_j^n - \kappa)\kappa \frac{V_{j+1}^n - V_{j-1}^n}{2\Delta x}\phi(t^n, x_j). \qquad (3.31)
\end{aligned}
$$

The first in the above expression can be controlled by $C(w_\eta, \rho_0)\Delta x$, and the second converges to

$$
- \int_0^{+\infty} \int_{-\infty}^{+\infty} \operatorname{sgn}(\rho_j^n - \kappa)\kappa V_x(t,x)\phi(t,x) dx dt, \qquad (3.32)
$$

providing the entropy inequality (3.6).

Chapter 4

Numerical simulations

In the original Hughes' model (Chapter 2) it is assumed that the overall density of the crowd is known by every individual and all walking costs of pedestrians are based on the current density. In order to include non-local effects which enable pedestrians react to the density of their surrounding area, convolution operator acting on the velocity term considered in mathematical models. In the previous chapter, we introduced the LWR model with non-local flux term which models reaction of drivers to downstream traffic flow. In this chapter, we give the formulation of non-local Hughes' model for pedestrian dynamics along with one-dimensional numerical simulations of both the original version of Hughes' model and the version with non-local flux term.

4.1 Numerical implementation of the Hughes' model

In this section, we analyze the numerical solution of the nonlinear conservation laws specifically the Hughes' model in one dimension with given initial condition and Dirichlet boundary conditions. The work is based on [4, 5, 11].
First, we recall the Hughes' model for macroscopic pedestrian flow in one space dimension

$$\rho_t(t,x) - \left(\rho(t,x)v(\rho(t,x))\frac{\phi_x}{|\phi_x|}\right)_x = 0, \quad x \in \Omega, t \geq 0, \tag{4.1a}$$

$$|\phi_x| = c(\rho(t,x)), \quad x \in \Omega, t \geq 0, \tag{4.1b}$$

in the spatial domain $\Omega =]-1,1[$. In the above equations, for $x \in \Omega$, $t \geq 0$, $\rho = \rho(t,x) \in [0,1]$ is the normalized crowd density, $v(\rho) = (1-\rho)$ is the velocity, $c(\rho) = 1/v(\rho)$ is the cost function and $f(\rho) = \rho(1-\rho)$ is the flux term. We assume that $c : [0,1[\to [1,+\infty[$ is a smooth function such that $c(0) = 1$ and $c'(\rho) \geq 0$ for $\rho \in [0,1[$. Equations (4.1) must

be completed with an initial condition such that

$$\rho(0,x) = \rho_0(x) \in BV(\mathbb{R}), \quad x \in \Omega. \tag{4.2}$$

We consider the Dirichlet boundary conditions as

$$\rho(t,-1) = \rho(t,1) = 0, \quad \phi(t,-1) = \phi(t,1) = 0, \quad t > 0 \tag{4.3}$$

where $x = \pm 1$ represent the exit locations. Given an initial datum (4.2) and homogeneous Dirichlet boundary conditions (4.3) we solve (4.1) in an iterative manner at each time step. The algorithm has two steps;

1. For a given ρ we solve the eikonal equation (4.1b) by the Fast Sweeping Method.
2. For a given ϕ we solve the nonlinear conservation law (4.1a) by using a Finite Volume Scheme with the Rusanov flux.

4.1.1 The fast sweeping algorithm for the eikonal equation (4.1b)

In this subsection, we explain the algorithm 1 which is used in order to solve the eikonal-type equation (4.1b). The method is given in [11]. In our case the model is only in one dimension but reader may refer to [11] for the generalized version of the method. Godunov upwind difference scheme used to discretize the partial differential equation at interior grid points of the spatial domain. The upwind differencing at the interior grid point i reads as

$$[(\phi_i^h - \phi_{xmin}^h)^+]^2 = c(\rho_i)^2 h^2, \quad i = 2, ..., N-1, \tag{4.4}$$

where $\phi_i^h = \phi(x_i)$, $\quad \phi_{xmin}^h = \min(\phi_{i-1}^h, \phi_{i+1}^h)$ and

$$(\phi_i^h - \phi_{xmin}^h)^+ = \begin{cases} \phi_i^h - \phi_{xmin}^h, & \phi_i^h - \phi_{xmin}^h > 0 \\ 0, & \phi_i^h - \phi_{xmin}^h \leq 0 \end{cases}$$

In order to enforce the boundary conditions $\phi(\pm 1) = 0$ we assign exact values at boundary grid points $x = \pm 1$. At the interior grid points we assign sufficiently large positive values which will be updated later.

At each grid point x_i whose value is not fixed during the initialization, we compute the solution $\bar{\phi}$ of (4.13) from the current values of its neighbors $\phi_{i\pm1}^h$. Then we update the distance value at grid i as

$$\phi_i^{new} = \min\{\min\{\phi_{i-1}, \phi_{i+1}\} + c(\rho_i)h, \phi_i\}$$

For the final step to solve (4.13) we use two Gauss-Seidel iterations with 2 sweeping orderings,

$$i = 1 : N, \quad i = N : 1$$

since there are only two directions for the characteristics in one dimension, i.e. from left to right and from right to left.

Algorithm 1 The fast sweeping algorithm for the Hughes' model

procedure INITIALIZATION
    Assign exact values at grid points on the boundaries for $i = 1$ and $i = N$.
    Assign large positive values at interior grid points, for $i = 2, ..., N-1$.
end procedure

procedure DISCRETIZATION
    Use Godunov upwind difference scheme at interior grid points

$$[(u_i^h - u_{xmin}^h)^+]^2 = c(\rho_i)^2 h^2, \quad i = 2, ..., N-1,$$

    where $u_i^h = u(x_i)$, $u_{xmin}^h = \min(u_{i-1}^h, u_{i+1}^h)$ and $(x)^+ = \begin{cases} x, & x > 0, \\ 0, & x \leq 0. \end{cases}$
end procedure

procedure ITERATIONS
    For each interior grid x_i for $i = 2, ..., N-1$, compute the solution $\bar{u}$ by 2.
    Update u_i^h, as $u_i^{new} = \min\{u_i^{old}, \bar{u}\}$.
    Sweep the whole domain with the ordering $i = 1 : N$.
    Sweep the whole domain with the ordering $i = N : 1$.
end procedure

4.1.2 Rusanov scheme for the solution of (4.1a)

Once we have the solution for the eikonal equation (4.1b), the next step is to construct the solutions for (4.1a) by using a finite volume scheme with the Rusanov flux as it is described in [4]. In this subsection we describe the algorithm 2 which solves numerically the equation (4.1a).

We divide the domain $\Omega =]-1, 1[$ in to $N-1$ uniform cells $I_i = [x_{i-1/2}, x_{i+1/2}]$ with $\Delta x = \frac{2}{N-1}$ and $x_i = i\Delta x$, $i = 1, ..., N-1$ are the center points of the cells.

We set $k_{i\pm1/2} = sgn(\phi_x^n(x_{i\pm1/2}))$ where

$$\phi_x^n(x_{i+1/2}) \simeq \frac{\phi^n(x_{i+1}) - \phi^n(x_i)}{\Delta x}.$$

Here the superscript n denotes the iteration in time.

For the numerical flux we use the following Rusanov scheme

$$h^n_{i+1/2} = h(\rho^n_i, \rho^n_{i+1}) = \frac{1}{2}(f(\rho^n_i) + f(\rho^n_{i+1})) + \frac{1}{2}\max\{|f'(\rho^n_i)|, |f'(\rho^n_{i+1})|\}(\rho^n_i - \rho^n_{i+1}) \quad (4.5)$$

which is known to be robust.

We ensure the monotonicity of the scheme by transposing the arguments when $k_{i+1/2}$

Algorithm 2 The finite volume scheme for the Hughes' model

1: **procedure** INITIALIZATION
2: Divide the domain Ω into $N-1$ uniform cells.
3: Specify the grid point locations, i.e. $x_i = i\Delta x$, $i = 1, ..., N-1$ are the center points of the cells.
4: Initialize the time $n = 0$.
5: Set the initial flux as 0.
6: Calculate the initial mass as $\rho_i \times h$, where h is the grid size.
7: **end procedure**

1: **procedure** ITERATIONS
2: **while** current mass is more than 99% of the initial mass **do**
3: Calculate $k_{i\pm1/2} = sgn(\phi^n_x(x_{i\pm1/2}))$ where $\phi^n_x(x_{i+1/2}) \simeq \frac{\phi^n(x_{i+1}) - \phi^n(x_i)}{\Delta x}$. Here Algorithm 1 is used to solve the eikonal equation.
4: Update the new flux according to 3 given by the Rusanov scheme (4.5).
5: Calculate the upper bound for Δt by using (4.8) and set Δt accordingly.
6: Update ρ_i by (4.7).
7: Calculate the current mass.
8: **end while**
9: **end procedure**

1: **procedure** PLOTTING
2: Store the final time T_f and the density ρ_{new} after while loop.
3: Plot the density profile.
4: **end procedure**

changes its sign,

$$h_{j+1/2} = \begin{cases} h(\rho^n_i, \rho^n_{i+1}), & if \quad k_{i+1/2} \le 0, \\ h(\rho^n_{i+1}, \rho^n_i), & if \quad k_{i+1/2} > 0. \end{cases} \quad (4.6)$$

Finally, we update ρ_i at each time iteration by

$$\rho^{n+1}_i = \rho^n_i - \frac{\Delta t^n}{\Delta x}(k_{i+1/2}h_{i+1/2} - k_{i-1/2}h_{i-1/2}) \quad (4.7)$$

where $\Delta t^n = t^{n+1} - t^n$ is chosen to satisfy the following CFL (Courant-Friedrichs-Lewy) condition

$$\Delta t^n < 0.5\frac{\Delta x}{\max\{\max_j\{|f'(\rho^n_j)|, |\dot{\xi}^n|\}\}} \quad (4.8)$$

where $|\dot{\xi}^n|$ is estimated by each time step by taking the derivative of (2.24) which gives,

$$\dot{\xi(t)}(c(\rho^-) + c(\rho^+)) = -\int_{-1}^{\xi(t)} c(\rho(t,y))_t dy + \int_{\xi(t)}^{1} c(\rho(t,y))_t dy. \tag{4.9}$$

From the above equality (4.9) we obtain the upper bound as

$$|\dot{\xi^n}| \leq \frac{1}{2}|\sum_j (1 - \rho_j^n - \rho_{j+1}^n)(c(\rho_j^n) - c(\rho_{j+1}^n))|. \tag{4.10}$$

In the inequality (4.8), the coefficient 0.5 is chosen to avoid interactions of ξ^n with the cell boundaries since at each time step $\xi^n = \xi(t)$ is forced to be located at the middle of the cell it belongs to.

4.2 Numerical implementation of the Hughes' model with non-local velocity term

In this section, we give the formulation of the Hughes' model for pedestrian flow with non-local flux term and we analyze the numerical solution of it in one dimension with given initial conditions and Dirichlet boundary conditions.
We start by defining the non-local Hughes' model for pedestrian flow in one space dimension

$$\rho_t(t,x) + \Big(\rho(t,x)v(\rho(t,x) * \omega_\eta(x,\eta))\Big)_x = 0, \quad x \in \Omega, t \geq 0, \tag{4.11a}$$

$$|\phi_x| = c(\rho(t,x)) = \frac{1}{v(\rho(t,x) * \omega_\eta(x,\eta))}, \quad x \in \Omega, t \geq 0, \tag{4.11b}$$

$$\rho(0,x) = \rho_0(x), \quad x \in \Omega, \tag{4.11c}$$

$$\rho(t,-1) = \rho(t,1) = 0, \quad \phi(t,-1) = \phi(t,1) = 0, \quad t > 0. \tag{4.11d}$$

where $\Omega =]-1,1[$ is the spatial domain and $\eta > 0$. Above, the convolution kernel $\omega_\eta \in \mathbf{C}^1([0,\eta];\mathbb{R}^+)$ is a non-increasing function such that $\int_{-\eta}^{\eta} \omega_\eta(x)dx = 1$. In the numerical simulations we used different kernels in order to study the effects of the convolution kernel to the evacuation time. The convolution product in (4.11a) is defined as

$$\rho * w_\eta(t,x) = \int_x^{x+\eta} \rho(t,y) w_\eta(y-x) dy. \tag{4.12}$$

Moreover, in the above equations, $\rho = \rho(t,x) \in [0,1]$ is the normalized crowd density, $v(\rho) = (1-\rho)$ is the velocity, $c(\rho) = 1/v(\rho(t,x) * \omega_\eta(x,\eta))$ is the cost function and $f(\rho) = \rho(1-\rho)$ is the flux term. The two exit points are located in the $x = \pm 1$. The methods that are used to implement the solution of the problem (4.17) are the same as

the methods that were used for the original Hughes' model in one space dimension (4.1). Therefore, there are two main steps;

1. For a given ρ we solve the eikonal equation (4.11b) by the Fast Sweeping Method. Here, the cost function is considered as $c(\rho * \omega_\eta)$ instead of $c(\rho)$.
2. For a given ϕ we solve the nonlinear conservation law (4.11a) by using a finite Volume Scheme with the Rusanov flux.

4.2.1 The fast sweeping algorithm for the eikonal equation (4.11b)

In this subsection, we explain the algorithm 3 which is used to solve the eikonal-type equation (4.11b). The method is one dimensional case proposed in in [11]. Godunov upwind difference scheme used to discretize the partial differential equation at interior grid points of the spatial domain.

Algorithm 3 The fast sweeping algorithm for the non-local Hughes' model

procedure INITIALIZATION
  Assign exact values at grid points on the boundaries for $i = 1$ and $i = N$.
  Assign large positive values at interior grid points, for $i = 2, ..., N-1$.
  Calculate the convolution product $\rho_i * \omega_{\eta_i}$ for a given ρ_0.
  Update ρ_i with the convolution product value $\rho_i * \omega_{\eta_i}$ in order to calculate the cost function $c(\rho_i * \omega_{\eta_i}) = 1/v(\rho_i * \omega_{\eta_i})$.
end procedure

procedure DISCRETIZATION
  Use Godunov upwind difference scheme at interior grid points

$$[(u_i^h - u_{xmin}^h)^+]^2 = c(\rho_i * \omega_{\eta_i})^2 h^2, \quad i = 2, ..., N-1,$$

  where $u_i^h = u(x_i)$, $\quad u_{xmin}^h = \min(u_{i-1}^h, u_{i+1}^h)$ and $(x)^+ = \begin{cases} x, & x > 0 \\ 0, & x \leq 0 \end{cases}$
end procedure

procedure ITERATIONS
  For each interior grid x_i for $i = 2, ..., N-1$, compute the solution $\bar{u}$ by 2.
  Update u_i^h, as $u_i^{new} = \min\{u_i^{old}, \bar{u}\}$.
  Sweep the whole domain with the ordering $i = 1 : N$.
  Sweep the whole domain with the ordering $i = N : 1$.
end procedure

The upwind differencing at the interior grid point i reads as

$$[(\phi_i^h - \phi_{xmin}^h)^+]^2 = c(\rho_i * \omega_{\eta_i})^2 h^2, \quad i = 2, ..., N-1, \tag{4.13}$$

where $\phi_i^h = \phi(x_i)$, $\quad \phi_{xmin}^h = \min(\phi_{i-1}^h, \phi_{i+1}^h)$ and

$$(\phi_i^h - \phi_{xmin}^h)^+ = \begin{cases} \phi_i^h - \phi_{xmin}^h, & \phi_i^h - \phi_{xmin}^h > 0 \\ 0, & \phi_i^h - \phi_{xmin}^h \leq 0 \end{cases}$$

In order to enforce the boundary conditions $\phi(\pm 1) = 0$ we assign exact values at boundary grid points $x = \pm 1$. At the interior grid points we assign sufficiently large positive values which will be updated later.

At each grid point x_i whose value is not fixed during the initialization, we compute the solution $\bar{\phi}$ of (4.13) from the current values of its neighbors $\phi_{i\pm 1}^h$. Then we update the distance value at grid i as

$$\phi_i^{new} = \min\{\min\{\phi_{i-1}, \phi_{i+1}\} + c(\rho_i * \omega_{\eta_i})h, \phi_i\}$$

For the final step to solve (4.13) we use two Gauss-Seidel iterations with 2 sweeping orderings,

$$i = 1 : N, \quad i = N : 1$$

since there are only two directions for the characteristics in one dimension, i.e. from left to right and from right to left.

There is only a small difference between the algorithms 1 and 3. In the original Hughes' model given by (4.1), it is assumed that the global distribution of all other individuals $\rho(t, x)$ is known to every pedestrian. By taking ρ_i as the input of the cost function $c(\rho_i)$ in the equation (4.13) we consider all walking costs based on the current density.

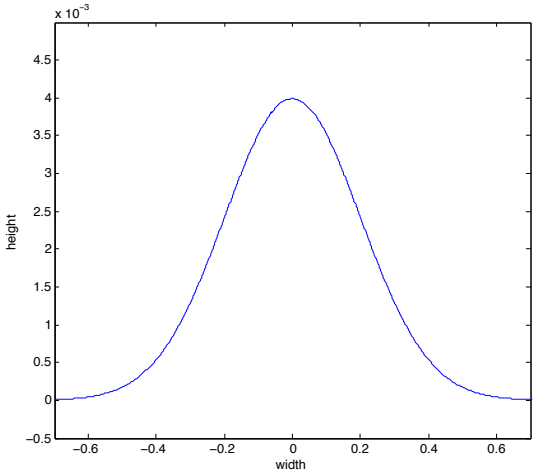

FIGURE 4.1: Gaussian convolution kernel

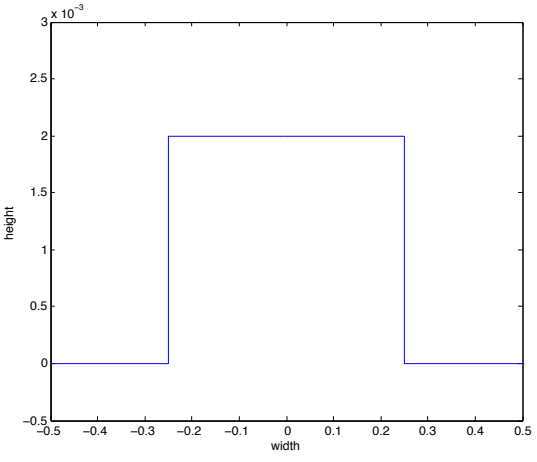

FIGURE 4.2: Rectangular convolution kernel

It means that pedestrians are able to react to changes in the global density. But in the practical situations, instead of complete perception of the global density, partial

knowledge of the density limited to the neighborhood of the pedestrian is more realistic. In order to model the limited perception of the density we took the cost function in (4.13) as $c(\rho_i * \omega_{\eta_i})$ where ω_{η_i} is the convolution kernel.
We consider first $\omega_{\eta,Gau}$ as a Gaussian kernel;

$$\omega_{\eta,Gau}(x,\eta) = \frac{1}{\eta} e^{-\frac{\pi(x-\mu)^2}{\eta^2}}. \tag{4.14}$$

The graph of a Gaussian function is a characteristic symmetric *bell curve* shape as in the figure 4.1. The parameter $\frac{1}{\eta}$ is the height of the curve's peak and the quantity defined as $\sigma := \frac{\eta}{\sqrt{2\pi}}$ controls the width of the *bell*. We consider the position of the center of the peak as 0, i.e. we use a symmetric Gaussian kernel. In our simulations, x is the domain $\Omega =]-1, 1[$, and σ values are ranging from 0.01 to 1.0.
Moreover, we considered a rectangular convolution kernel $\omega_{\eta,rect}(x,\eta)$ (see figure 4.2) defined as

$$\omega_{\eta,rect}(x,\eta) = \begin{cases} 0, & if \quad |x| > \frac{\eta}{2}, \\ \frac{1}{2\eta}, & if \quad x = \frac{\eta}{2}, \\ \frac{1}{\eta}, & if \quad |x| < \frac{\eta}{2}. \end{cases} \tag{4.15}$$

where the parameter η is the horizontal width of the rectangular. We may write (4.15) as

$$\omega_{\eta,rect}(x,\eta) = \frac{1}{\eta}\chi_{\{-\eta/2,\eta/2\}}(x).$$

Thus the convolution product takes the form,

$$\rho * w_{\eta,rect}(t,x) = \frac{1}{\eta}\int_{x-\eta/2}^{x+\eta/2} \rho(t,y)dy \tag{4.16}$$

In the simulations η is ranging from 0 to 1.5.

4.2.2 Rusanov scheme for the solution of (4.11a)

In this subsection we give the algorithm 4 which solves the equation (4.11a). We refer to the section 4.1.2 for more explanation. Only difference between the algorithms 2 and 4 is that in the second one the cost function is taken as $c(\rho_i * \omega_{\eta_i})$ where ω_{η_i} is the convolution kernel. As it is defined in the previous section, we considered both the Gaussian kernel and the rectangular kernel for the simulations. For this reason, as a part of the *Initialization* process in the algorithm 4, we specified σ value for the Gaussian kernel and the width η for the rectangular kernel.

Algorithm 4 The finite volume scheme for the non-local Hughes' model

procedure INITIALIZATION
  Divide the domain Ω into $N-1$ uniform cells.
  Specify the grid point locations, i.e. $x_i = i\Delta x$, $i = 1, ..., N-1$ are the center points of the cells.
  Initialize the time $n = 0$.
  Set the initial flux as 0.
  Calculate the initial mass as $\rho_i \times h$, where h is the grid size.
  Specify σ value for the Gaussian kernel and the width η value for the rectangular kernel.
end procedure

procedure ITERATIONS
  while current mass is more than 99% of the initial mass **do**
    Calculate $k_{i\pm1/2} = sgn(\phi_x^n(x_{i\pm1/2}))$ where $\phi_x^n(x_{i+1/2}) \simeq \frac{\phi^n(x_{i+1}) - \phi^n(x_i)}{\Delta x}$. Here, Algorithm 3 is used to solve the eikonal equation.
    Update the new flux according to 3 given by the Rusanov scheme (4.5).
    Calculate the upper bound for Δt by using (4.8) and set Δt accordingly.
    Update ρ_i by (4.7).
    Calculate the current mass.
  end while
end procedure

procedure PLOTTING
  Store the final time T_f and the density ρ_{new} after while loop.
  Plot the density profile.
end procedure

4.3 Results

In this section we present the results obtained for three different initial data for the density ρ. Initial data are selected so that the initial masses are all same for three of the initial data sets. First initial datum $\rho_{0,1}$ we considered is of Riemann type;

$$\rho_1(0,x) = \rho_{0,1} = \begin{cases} 0.1, & if \quad x \leq 0 \\ 0.7, & if \quad x > 0 \end{cases} \tag{4.17}$$

Second initial datum $\rho_{0,2}$ is of more general type;

$$\rho_2(0,x) = \rho_{0,2} = \begin{cases} 0.8, & if \quad -0.8 \leq x < -0.5, \\ 0.6, & if \quad -0.3 \leq x \leq 0.3, \\ 0.4, & if \quad 0.4 \leq x < 0.9, \\ 0, & elsewhere \end{cases} \tag{4.18}$$

The last initial datum $\rho_{0,3}$ we considered is the following;

$$\rho_3(0,x) = \rho_{0,3} = \begin{cases} 0.85, & if \quad -1 \leq x \leq -0.2, \\ 0, & if \quad -0.3 < x \leq 0.6, \\ 0.3, & if \quad 0.6 < x \leq 1 \end{cases} \tag{4.19}$$

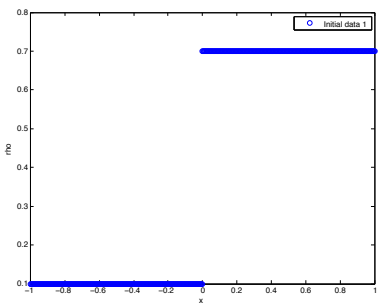

FIGURE 4.3: $\rho_{0,1}$

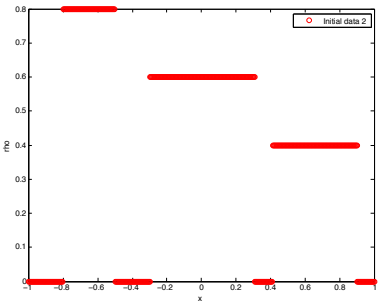

FIGURE 4.4: $\rho_{0,2}$

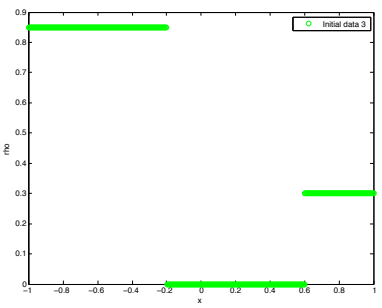

FIGURE 4.5: $\rho_{0,3}$

In the simulations, first we implemented the numerical solution of the Hughes' model for pedestrian crowd dynamics with the initial data shown in the figures 4.6, 4.7 and 4.12 and homogeneous Dirichlet boundary conditions. Then, a localized smooth variant of the same model was considered.

It is observed that a convolution term in the cost function allows pedestrians to move according to knowledge of the density around them rather than the perception of the global density. In other words, by considering a Gaussian or a rectangular type of kernel, decisions of pedestrians will get affected more by the changes in the density of the closer areas to themselves than the global changes. This is a more realistic approach for large groups of pedestrians.

Based on a given initial data, we are able to obtain the best σ or η value for the convolution kernels which affects the further movements of pedestrians. For the Gaussian kernel the range we considered for the σ value is from 0.01 to 1. The optimal values for σ which gives the shortest evacuation time are 0.2 for $\rho_{0,1}$, 0.1 for $\rho_{0,2}$ and 0.03 for $\rho_{0,3}$. On the other hand, the optimal width values η for the rectangular kernel are 0.9 for $\rho_{0,1}$, $0.9 - 1.0 - 1.1$ for $\rho_{0,2}$ and 0.1 for $\rho_{0,3}$ ant the range of η considered is from 0 to 1.5.

The figure 4.6 shows the one-dimensional simulation of Hughes' model (4.1) with $\rho_{0,1}$. Evacuation time represents the time required to empty 99% of the initial mass. The figures 4.8 and 4.10 shows the simulations with the same initial data considering respectively a Gaussian and a rectangular kernel. The parameters $\sigma = 0.2$ and $\eta = 0.9$ are the values at which the evacuation time is shortest. We called them as *optimal values*. We explain the figures 4.7, 4.9, 4.11 for $\rho_{0,2}$ and the figures 4.12, 4.13, 4.14 for $\rho_{0,3}$ similarly.

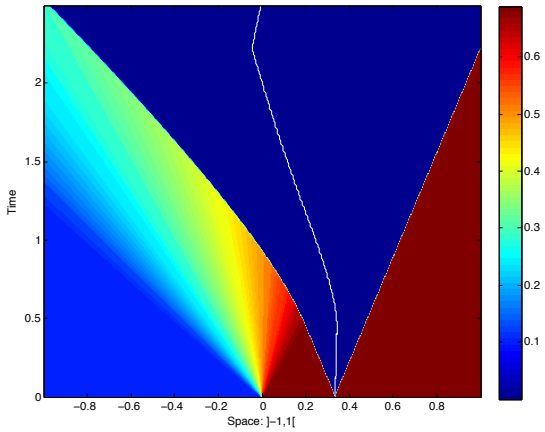

FIGURE 4.6: $\rho_{0,1}$ without convolution
Time = 2.4975

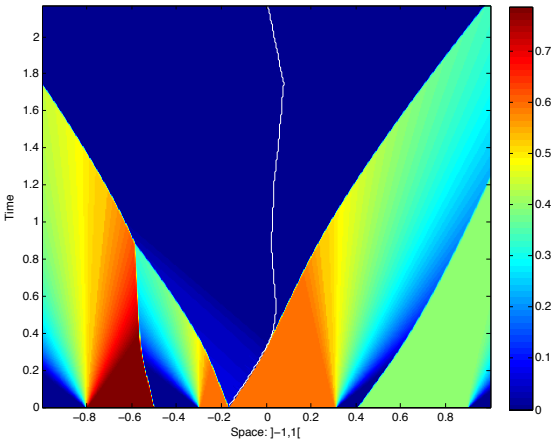

FIGURE 4.7: $\rho_{0,2}$ without convolution
Time = 2.1698

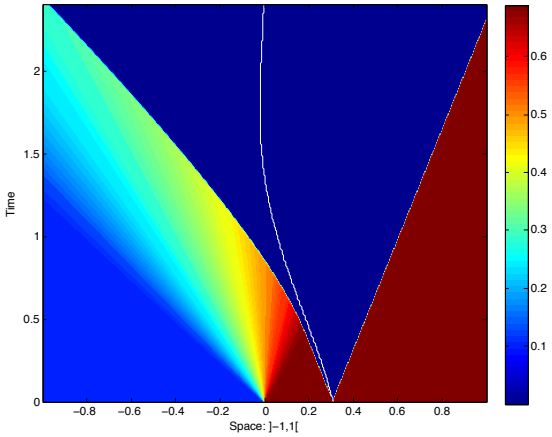

FIGURE 4.8: $\rho_{0,1}$ with $\omega_{\eta,Gauss}$
$\sigma = 0.2$, Time = 2.4065

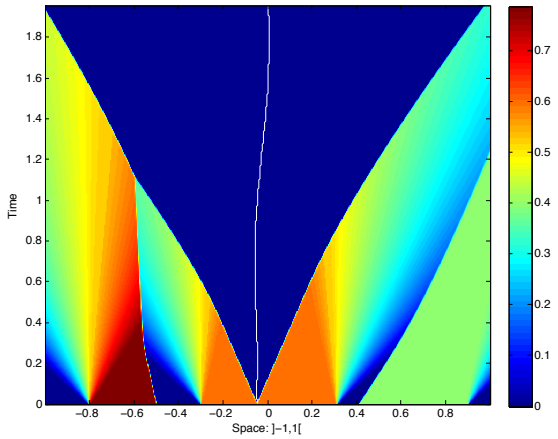

FIGURE 4.9: $\rho_{0,2}$ with $\omega_{\eta,Gauss}$
$\sigma = 0.1$, Time = 1.9576

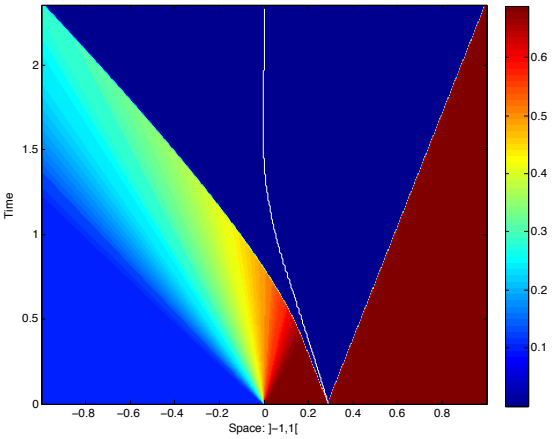

FIGURE 4.10: $\rho_{0,1}$ with $\omega_{\eta,rect}$
$\eta = 0.9$, Time = 2.3588

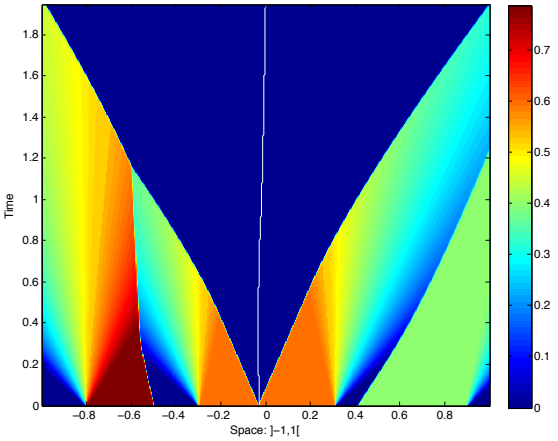

FIGURE 4.11: $\rho_{0,2}$ with $\omega_{\eta,rect}$
$\eta = 0.9 - 1.0 - 1.1$, Time = 1.9476

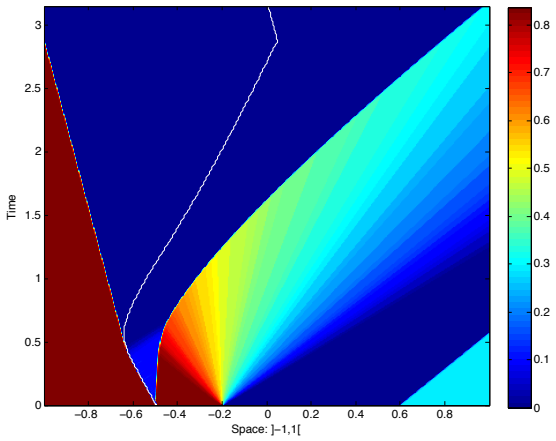

FIGURE 4.12: $\rho_{0,3}$ without convolution, Time = 3.1531

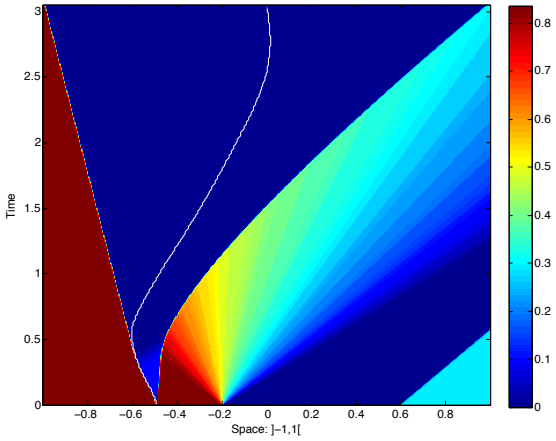

FIGURE 4.13: $\rho_{0,3}$ with $\omega_{\eta,Gauss}$ $\sigma = 0.03$, Time = 3.0544

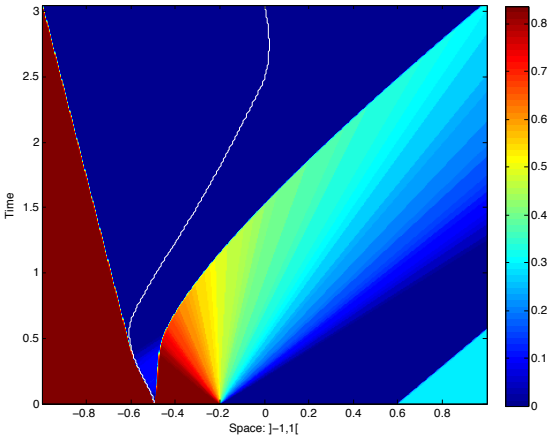

FIGURE 4.14: $\rho_{0,3}$ with $\omega_{\eta,rect}$ $\eta = 0.1$, Time = 3.0524

Moreover, in the figures 4.15, 4.17, 4.19, 4.16, 4.18 and 4.20 we see the plots of evacuation time versus change in either σ or η values. In the graphs, horizontal lines show evacuation time of local version of Hughes' model. It is seen from the figures that there exist an optimal value for the non-local model which makes evacuation time shorter than the one with the original model. However, that value is not the same for all types of initial data.

In the tables 4.1 and 4.2 we see the change in evacuation time depending on the width of kernel considered. We can compare evacuation time for all three of the initial data from the figures 4.1 and 4.2. We can deduce from the figures that optimal time is highly dependent on the initial data. Although, we have taken the initial mass as same for all three different initial data, because of initial distribution of mass the evacuation time is different for all three of them.

In addition, as we see in the figure 4.21, width of $6 \times \sigma$ of the Gaussian kernel covers

TABLE 4.1: Evacuation time with respect to σ of the Gaussian kernel

	Evacuation Time		
σ	$\rho_{0,1}$	$\rho_{0,2}$	$\rho_{0,3}$
0.01	2.4926	2.1613	3.1144
0.02	2.4882	2.1526	3.0734
0.03	2.4882	2.1427	**3.0544**
0.04	2.4834	2.1336	3.0914
0.05	2.4822	2.1096	3.1584
0.06	2.4804	2.0766	3.2244
0.07	2.4752	2.0386	3.2883
0.08	2.4752	2.0066	3.3043
0.09	2.4716	1.9786	3.3063
0.1	2.4682	**1.9576**	3.3133
0.2	**2.4065**	1.9606	3.7512
0.3	2.4236	1.9646	4.2511
0.4	2.5874	1.9696	4.8380
0.5	2.7095	1.9796	5.2320
0.6	2.7921	1.9846	5.2709
0.7	2.8461	1.9896	5.2709
0.8	2.8791	1.9946	5.2709
0.9	2.9061	1.9946	5.2709
1.0	2.9261	1.9986	5.2709
without conv	2.4975	2.1698	3.1531

TABLE 4.2: Evacuation time with respect to η of the rectangular kernel

	Evacuation Time		
η	$\rho_{0,1}$	$\rho_{0,2}$	$\rho_{0,3}$
0	2.4975	2.1698	3.1531
0.1	2.4856	2.1460	**3.0524**
0.2	2.4752	2.0936	3.1934
0.3	2.4682	1.9896	3.2913
0.4	2.4613	1.9476	3.3563
0.5	2.4517	1.9606	3.5243
0.6	2.4417	1.9666	3.6793
0.7	2.4261	1.9606	3.8052
0.8	2.3898	1.9556	3.9262
0.9	**2.3588**	**1.9476**	4.0762
1.0	2.4055	**1.9476**	4.3241
1.1	2.4804	**1.9476**	4.5841
1.2	2.5533	1.9506	4.8110
1.3	2.6235	1.9556	5.0240
1.4	2.6875	1.9646	5.2180
1.5	2.7513	1.9746	5.2709
without conv.	2.4975	2.1698	3.1531

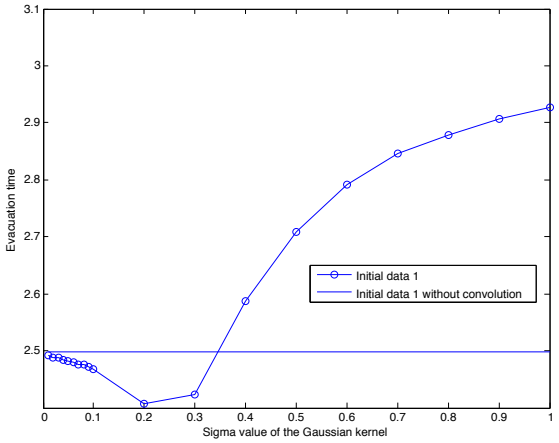

FIGURE 4.15: $\rho_{0,1}$, Gaussian kernel

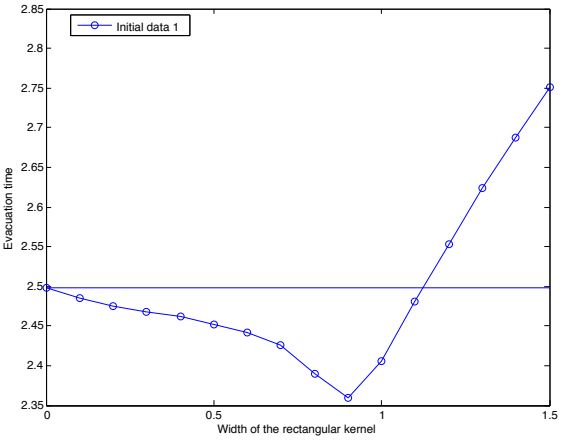

FIGURE 4.16: $\rho_{0,1}$, rectangular kernel

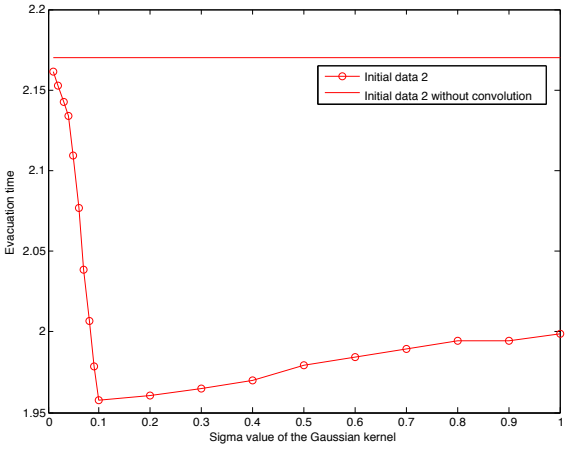

FIGURE 4.17: $\rho_{0,2}$, Gaussian kernel

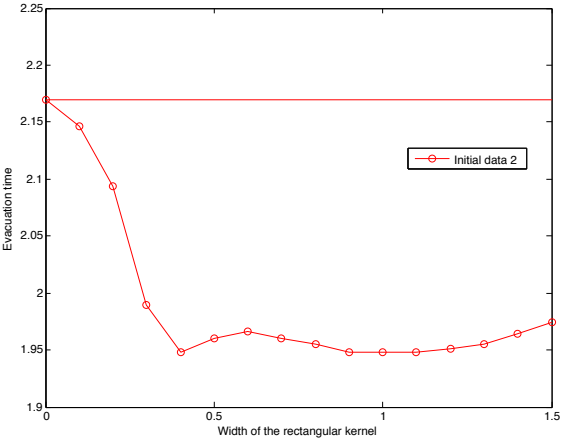

FIGURE 4.18: $\rho_{0,2}$, rectangular kernel

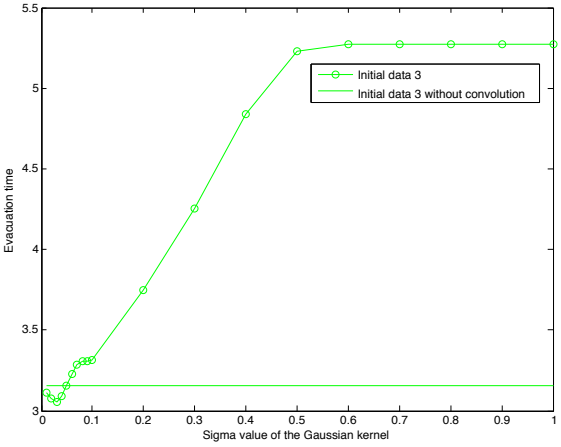

FIGURE 4.19: $\rho_{0,3}$, Gaussian kernel

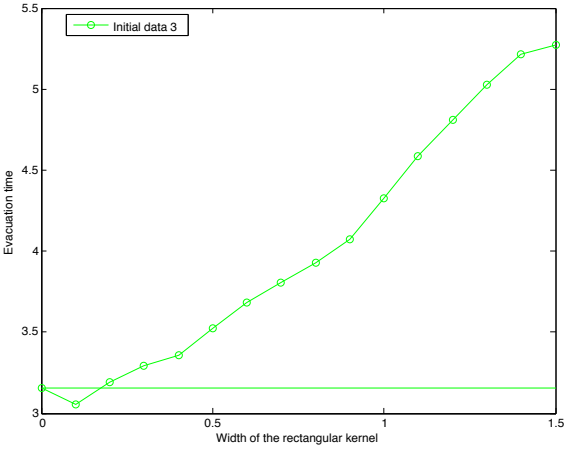

FIGURE 4.20: $\rho_{0,3}$, rectangular kernel

almost same width of η of the rectangular kernel. We took the values of σ and η which gives the optimal time for $\rho_{0.2}$.

The MATLAB codes which are used in this section can be found in the Appendix A.

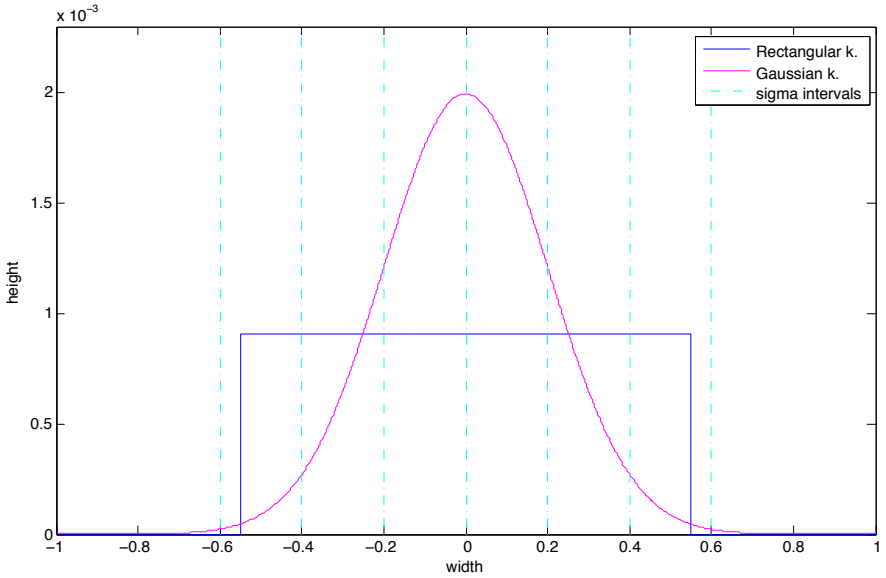

FIGURE 4.21: Comparison of width of Gaussian kernel and width of rectangular kernel, $\sigma = 0.1$, $\eta = 1.1$

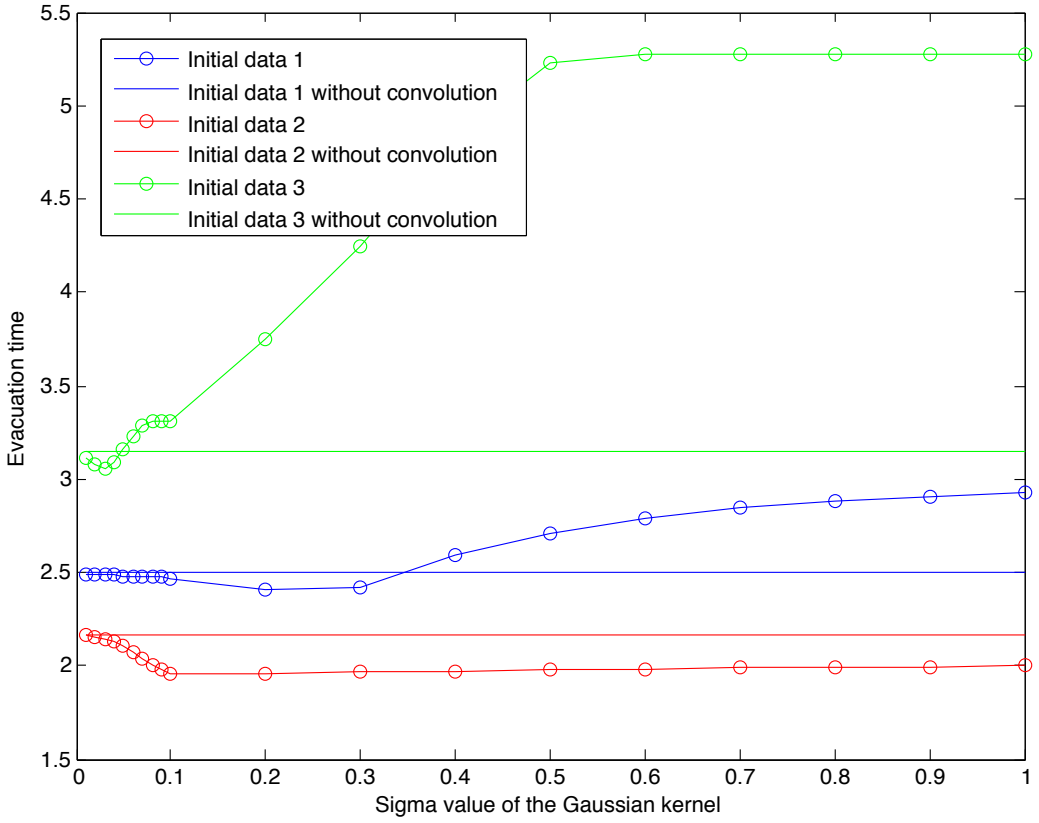

FIGURE 4.22: Comparison of evacuation time with respect to initial data in the case of a Gausssian kernel

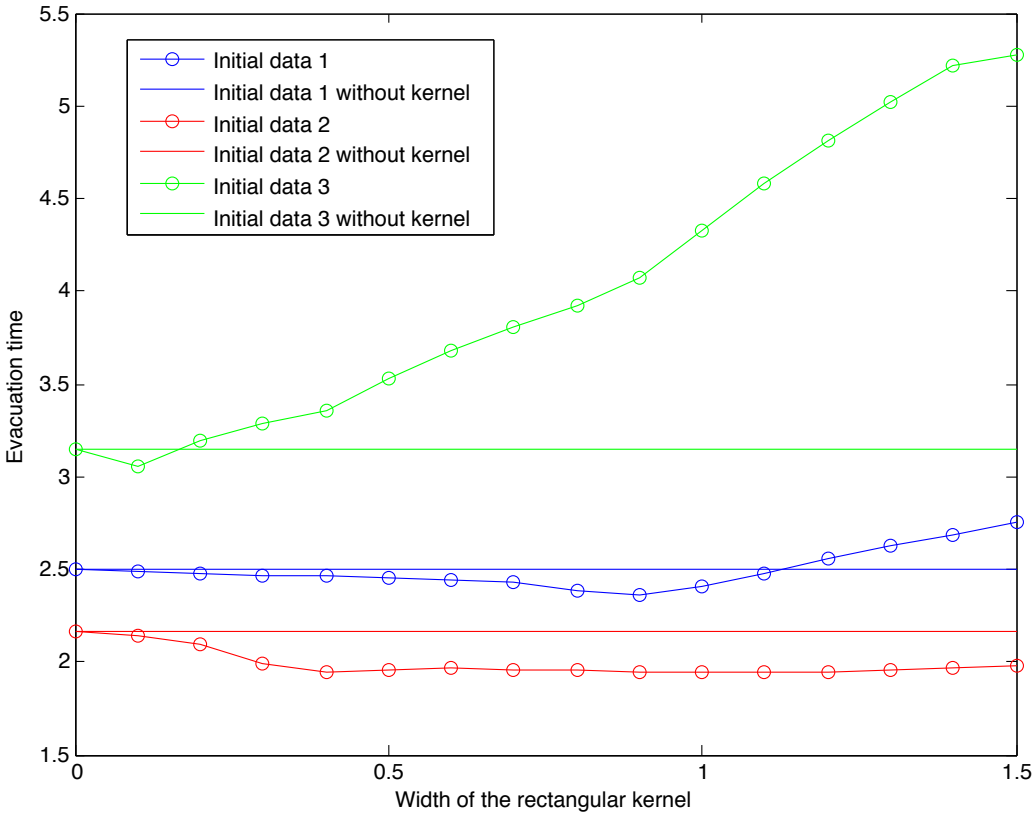

FIGURE 4.23: Comparison of evacuation time with respect to initial data in the case of a rectangular kernel

Chapter 5

Conclusion and future work

Main aim of the thesis is the study of the non-local version of the Hughes' model. We implemented the numerical solutions of both the original and the non-local versions of one-dimensional Hughes' model by using MATLAB environment. Effect of the convolution kernels to the evacuation time was investigated. We considered two different functions as convolution kernel in the simulations. They are the Gaussian function given by (4.14) and a rectangular pulse function given by (4.15).

Based on our observations, we proposed an alternative version to the non-local model considering some modifications of the rectangular convolution kernel. In the previous simulations (Chapter 4) symmetric rectangular kernel was used. Here we consider non-symmetric rectangular kernel modeling the behavior of looking at the direction of closer exit more than the other direction. Another modification we make is that width of the rectangular kernel is decreasing near exits, approaching dirac-delta function on the exit points $x = \pm 1$. This is a reasonable assumption since at the points which are closer to the exits, by using a rectangular kernel with a constant width we have to take into account the density information of the points beyond the exits at $x = \pm 1$.

We refer to the non-local model with initial and homogeneous Dirichlet boundary conditions given by (4.17) and the symmetric rectangular convolution kernel given by (4.14). For a given turning point $\xi \in]-1, 1[$, we define the shift towards an exit point from the location of a pedestrian as

$$x_{shift}(x, \xi) = \begin{cases} -\delta, & x < \xi, \\ +\delta, & x > \xi. \end{cases} \tag{5.1}$$

where $x \in \Omega =]-1, 1[$ and $\delta > 0$. For the sake of simplicity we take $\delta = \eta/2$, where η is width of the rectangular convolution kernel. Thus, the center of the convolution kernel

x_{center} becomes

$$x_{center}(x,\xi) = x + x_{shift}(x,\xi) = \begin{cases} x - \frac{\eta}{2}, & x < \xi, \\ x + \frac{\eta}{2}, & x > \xi. \end{cases} \tag{5.2}$$

We define the convolution product on both sides of the turning point as

$$\rho * \omega_{\eta,rect}(x,\eta) = \rho_\xi(x) = \begin{cases} \frac{1}{\eta}\int_{x-\eta}^{x} \rho(z)dz, & x < \xi, \\ \frac{1}{\eta}\int_{x}^{x+\eta} \rho(z)dz, & x > \xi. \end{cases} \tag{5.3}$$

Moreover, ρ needs to be extended as 0 in $[-1-\eta,-1]$ and $[1,1+\eta]$ to define the above convolution product (5.3). In order to find the solution of the eikonal equation (4.11b) we need to have a turning point ξ such that

$$\int_{-1}^{\xi} c(\rho_\xi)dx = \int_{\xi}^{1} c(\rho_\xi)dx \tag{5.4}$$

for given parameters $\eta > 0$ and for $\rho(x) \in L^\infty(]-1,1[;[0,1])$. Note that the equation (5.4) depends ξ on implicitly. We define an auxiliary function such that

$$\varphi(\xi) = \int_{-1}^{\xi} c(\rho_\xi)dx - \int_{\xi}^{1} c(\rho_\xi)dx.$$

We know that the mapping

$$\xi \to \varphi(\xi) = \int_{-1}^{\xi} c(\rho_\xi)dx - \int_{\xi}^{1} c(\rho_\xi)dx$$

is a continuous quantity being sum of continuous functions. Notice that

$$\varphi(-1) = -\int_{-1}^{1} c(\rho_{-1})dx < 0, \quad \varphi(1) = \int_{-1}^{1} c(\rho_{+1})dx > 0.$$

If φ is strictly monotone, then there exits a unique solution to $\varphi(\xi) = 0$. Moreover, giving a proof of this argument can be a part of future work. Numerical simulations and possible extensions of the model such that $\eta \to 0$ as $x \to \pm 1$ can also be considered.

Appendix A

MATLAB codes

Eikonal equation solver for (4.1b)

```
%% STEP 1: Given rho, solve the eikonal equation by the fast sweeping method

function [k, turn] = eikonal(rho, N)
% h grid size
% N number off cells
% domain ]-1,1[
h = 2/(N-1);
u = zeros(N+1,1);
% cost function
cost = @(x) (1./(1-x));

%% assigning random big values to the grid points inside the domain
for i=2:N
    u(i) = 500;
end

%% first sweeping
for i=2:N
 u(i) = min( min ( u(i+1),u(i-1) )+ (cost(rho(i-1)))*h, u(i));
end

%% second sweeping
 for i=N:-1:2
    u(i) = min( min(u(i+1),u(i-1))+ (cost(rho(i-1)))*h, u(i));
 end

%% defining k
 k = -sign(u(2:N+1)-u(1:N));

%% turning point
 for i=1:N-1
     if k(i) ~= k(i+1)
    turn = i;
     end
 end
```

Eikonal equation solver for (4.11b) with a Gaussian kernel

```
%% STEP 1: Given rho, solve the eikonal equation by the fast sweeping method

function [k, turn, z] = eikonal_conv(rho, N, sigma)
% h grid size
% N number off cells
% domain interval ]-1,1[

h = 2/(N-1);
u = zeros(N+1,1);
cost = @(x) (1./(1-x));

%% assigning big values to the grid points inside the domain
for i=2:N
    u(i) = 500;
end
x = -1:h:1;

%% calculating the values for the Gaussian kernel
Gauss = normpdf (x, 0, sigma);
Gauss = Gauss./sum(Gauss);

%% convolution
z = conv(rho, Gauss, 'same');
rho = z;

%% first sweeping
for i=2:N
 u(i) = min( min ( u(i+1),u(i-1) )+ (cost(rho(i-1)))*h, u(i));
end

%% second sweeping
 for i=N:-1:2
    u(i) = min( min(u(i+1),u(i-1))+ (cost(rho(i-1)))*h, u(i));
 end

%% defining k
 k = -sign(u(2:N+1)-u(1:N));

%% turning point
 for i=1:N-1
     if k(i) ~= k(i+1);
    turn = i;
     end
 end
```

Eikonal equation solver for (4.11b) with a rectangular kernel

```
%% STEP 1: Given rho, solve the eikonal equation by the fast sweeping method

function [k, turn, z] = eikonal_rect(rho, N, width)
% h grid size
% N number off cells
% domain interval ]-1,1[
```

```
h = 2/(N-1);
u = zeros(N+1,1);
cost = @(x) (1./(1-x));

%% assigning big values to the grid points inside the domain
for i=2:N
    u(i) = 500;
end

x = -1:h:1;

%% calculating the values for the rectangular kernel
 Kernel = rectpuls(x, width);
 Kernel = Kernel./sum(Kernel);

%% convolution
z = conv(rho, Kernel, 'same');
rho = z;

%% first sweeping
for i=2:N
 u(i) = min( min ( u(i+1),u(i-1) )+ (cost(rho(i-1)))*h, u(i));
end

%% second sweeping
 for i=N:-1:2
    u(i) = min( min(u(i+1),u(i-1))+ (cost(rho(i-1)))*h, u(i));
 end

%% defining k
 k = -sign(u(2:N+1)-u(1:N));

%% turning point
 for i=1:N-1
     if k(i) ~= k(i+1);
    turn = i;
     end
 end
```

Solution to (4.1) with $\rho_{0,1}$ Riemann type initial data

```
%% STEP 2: Given u(solution to the eikonal eqn), solve the nonlinear conservation
law with Rusanov flux
% Riemann type initial data
close all
clear all
clc

%% defining functions
cost = @(x) (1 ./(1-x));
f = @(x) (x.*(1-x));
df = @(x) (1-2*x);
h = @(x,y) ((0.5*(f(x)+f(y)))+(0.5*(max(abs(df(x)),abs(df(y)))).*(x-y)));
N=1001; %% number of cells: N-1
```

```
%% coordinates of cell center and end points
xmax = 1;
xmin = -1;
x = linspace(xmin, xmax, N);
xcenter = 0.5*(x(1:N-1)+x(2:N));
delta_x = x(2)-x(1); %% cell size
t=0; %% initial time

%% defining rho
rhoL=0.1;
rhoR=0.7;
for i=1: N-1
    if i <= (N-1)/2
        rho(i,1) = rhoL;
    elseif i> (N-1)/2
        rho(i,1) = rhoR;
    end
end

RHO = rho;
flux = zeros(1,N);
%% initial mass
mass0 = delta_x * sum(rho);
%%%% necessary only if convolution term is considered in the cost function
%% specify the sigma value for the Gaussian
%% sigma = 0.2;

      j=1; %time
      mass = mass0;
      t=0;
      T=t;
while mass >= 0.01*(mass0) %% condition for 99% of the crowd is getting emptied

    %% calling eikonal function to get k
    [k, turn] = eikonal(rho,N);
    %%%% [k, turn, conv_rho] = eikonal_conv(rho,N,sigma);
    % in the case that convolution term is considered
     k = k';

    %% update flux according to k value
    for i=2:turn
        flux(i) = h(rho(i),rho(i-1));
    end
    for i=turn+1:N-1
        flux(i) = h(rho(i-1), rho(i));
    end
    flux(1) = f(rho(1));
    flux(N) = f(rho(N-1));
    flux = k .*flux;

    %% upper bound for delta t
    ub = (0.5)*abs(sum((1-rho(1:N-2)-rho(2:N-1)).*(cost(rho(1:N-2))-cost(rho(2:N-1)))));
    y = df(rho);
    denominator = max(max(abs(y)),ub);
```

```
    delta_t = (0.4999)*(delta_x)/(denominator);

    %% rho update
    rho_new = rho - (delta_t/delta_x)*(flux(2:N)-flux(1:N-1))';
    RHO = [RHO rho_new];
    rho = rho_new;

    mass = delta_x*sum(rho);
    t = t + delta_t;
    T = [T t];
    tp(j) = turn; % turning points
    j= j+1;
end
    tp= (tp - (N-1)/2)./(N/2); % scaling for the turning points
    fprintf('iteration number : %d\n',t );
    %% ploting the solution
    figure(1)
        [C, h] =contourf (xcenter, T, RHO', 64);
        set(h, 'LineColor', 'none');
    %% plot the turning curve
        hold on
        plot(tp, T(2:j), 'w');
    ylabel('Time');
    xlabel('Space: ]-1,1[');
```

Solution to (4.17) with $\rho_{0,1}$ Riemann type initial data by considering a Gaussian kernel

```
%% Given u(soln to eikonal eqn), solve the nonlinear conservation law with Rusanov scheme
% Riemann type initial data
close all
clear all
clc

%% define functions
cost = @(x) (1 ./(1-x));
f = @(x) (x.*(1-x));
df = @(x) (1-2*x);
h = @(x,y) ((0.5*(f(x)+f(y)))+(0.5*(max(abs(df(x)),abs(df(y)))).*(x-y)));
N=1001; %% number of cells: N-1

%% coordinates of cell end points
xmax = 1;
xmin = -1;
x = linspace(xmin, xmax, N);
xcenter = 0.5*(x(1:N-1)+x(2:N));

delta_x = x(2)-x(1); %% cell size
t=0;                 %% initial time
Tf = 0.5;            %% final time

%% defining rho
rhoL=0.1;
rhoR=0.7;
for i=1: N-1
    if i <= (N-1)/2
```

```
        rho(i,1) = rhoL;
    elseif i> (N-1)/2
        rho(i,1) = rhoR;
    end
end
mass0 = delta_x*sum(rho);
RHO = rho;

%% specify the sigma value for the Gaussian
sigma = 0.2;
      tic
      t=0; %time
      j=1;
      T=t;
      mass=mass0;
while mass >= 0.01*mass0 %t <= Tf

    %% call eikonal function to get k
    [k, turn, conv_rho] = eikonal_conv(rho,N,sigma);
    k = k';

    %% update flux according to k value
    for i=2:turn
        flux(i) = h(rho(i),rho(i-1));
    end
    for i=turn+1:N-1
        flux(i) = h(rho(i-1), rho(i));
    end
    flux(1) = f(rho(1));
    flux(N) = f(rho(N-1));
    flux = k .*flux;

    %% upper bound for delta t
    y = df(rho);
    ub = (0.5)*abs(sum((1-rho(1:N-2)-rho(2:N-1)).*(cost(conv_rho(1:N-2))-cost(conv_rho(2:N-1)))));
    denominator = max(max(abs(y)),ub);
    delta_t = (0.4999)*(delta_x)/(denominator);

    %% rho update
    rho_new = rho-(delta_t/delta_x)*(flux(2:N)'-flux(1:N-1)');
    RHO = [RHO rho_new];
    rho = rho_new;

    %% mass update
    mass = delta_x*sum(rho);
    t = t + delta_t;
    T = [T t];
    tp (j) = turn; % turning point
    j= j+1;
end
toc
tp;
tp = (tp - (N-1)/2)./(N/2);
fprintf('Evacuation time: %d\n', t);
figure (1)
```

```
[C, h] =contourf(xcenter, T, RHO',64);
set(h, 'LineColor', 'none');
hold on
plot(tp, T(2:j), 'w');

ylabel('Time');
xlabel('Space: ]-1,1[');
```

Solution to (4.17) with $\rho_{0,1}$ Riemann type initial data by considering a rectangular

```
%% Given u(soln to eikonal eqn), solve the nonlinear conservation law with Rusanov scheme
% Riemann type initial data
close all
clear all
clc

%% define functions
cost = @(x) (1 ./(1-x));
f = @(x) (x.*(1-x));
df = @(x) (1-2*x);
h = @(x,y) ((0.5*(f(x)+f(y)))+(0.5*(max(abs(df(x)),abs(df(y)))).*(x-y)));
N=1001; %% number of cells: N-1

%% coordinates of cell end points
xmax = 1;
xmin = -1;
x = linspace(xmin, xmax, N);
xcenter = 0.5*(x(1:N-1)+x(2:N));

delta_x = x(2)-x(1); %% cell size
t=0;                 %% initial time
Tf = 0.5;            %% final time

%% defining rho
rhoL=0.1;
rhoR=0.7;
for i=1: N-1
    if i <= (N-1)/2
        rho(i,1) = rhoL;
    elseif i> (N-1)/2
        rho(i,1) = rhoR;
    end
end
mass0 = delta_x*sum(rho);
RHO = rho;

%% specify the width value for the rectangular kernel
width = 0.9;
      tic
      t=0; %time
      j=1;
      T=t;
      mass=mass0;
while mass >= 0.01*mass0 %t <= Tf
```

```
    %% call eikonal function to get k
    [k, turn, conv_rho] = eikonal_rect(rho,N,width);
    k = k';

    %% update flux according to k value
    for i=2:turn
        flux(i) = h(rho(i),rho(i-1));
    end
    for i=turn+1:N-1
        flux(i) = h(rho(i-1), rho(i));
    end
    flux(1) = f(rho(1));
    flux(N) = f(rho(N-1));
    flux = k .*flux;

    %% upper bound for delta t
    y = df(rho);
    ub = (0.5)*abs(sum((1-rho(1:N-2)-rho(2:N-1)).*(cost(conv_rho(1:N-2))-cost(conv_rho(2:N-1)))));
    denominator = max(max(abs(y)),ub);
    delta_t = (0.4999)*(delta_x)/(denominator);

    %% rho update
    rho_new = rho-(delta_t/delta_x)*(flux(2:N)'-flux(1:N-1)');
    RHO = [RHO rho_new];
    rho = rho_new;

    %% mass update
    mass = delta_x*sum(rho);
    t = t + delta_t;
    T = [T t];
    tp (j) = turn; % turning point
    j= j+1;
end
toc
tp;
tp = (tp - (N-1)/2)./(N/2);
fprintf('Evacuation time: %d\n', t);
figure (1)
[C, h] =contourf(xcenter, T, RHO',64);
set(h, 'LineColor', 'none');
hold on
plot(tp, T(2:j), 'w');

ylabel('Time');
xlabel('Space: ]-1,1[');
```

Bibliography

[1] Debora Amadori and Marco di Francesco. The one-dimensional Hughes model for pedestrian flow: Riemann-type solutions. *Acta Mathematica Scientia*, 32:259–280, January 2012.

[2] Sebastien Blandin and Paola Goatin. Well-posedness of a conservation law with non-local flux arising in traffic flow modeling. *Inria Sophia Antipolis*, March 2014.

[3] Benedetto Piccoli Emiliano Cristiani and Andrea Tosin. Multiscale modeling of pedestrian dynamics. *Springer*, 12, 2014.

[4] Paola Goatin and Matthias Mimault. The wave-front tracking algorithm for Hughes' model of pedestrian motion. *SIAM Journal on Scientific Computing (SISC)*, 35(3):B606–B622, 2013.

[5] Paola Goatin and Sheila Scialanga. The Lighthill-Whitham-Richards traffic flow model with non-local velocity: analytical study and numerical results. *Inria Sophia Antipolis*, page 36, February 2015.

[6] Roger L. Hughes. A continuum theory for the flow of pedestrians. *Transportation Research Part B: Methodological*, 36(6):507–535, July 2002.

[7] Roger L. Hughes. The flow of human crowds. *Annual Review of Fluid Mechanics*, 35:169–182, January 2003.

[8] Stephan Martin Jose A. Carrillo and Marie-Therese Wolfram. A local version of the Hughes model for pedestrian flow. January 2015.

[9] Pushkin Kachroo. Pedestrian dynamics: Mathematical theory and evacuation control. *CRC Press*, March 2009.

[10] Paola Goatin Nader el Khatib and Massimiliano D. Rosini. On entropy weak solutions of Hughes' model for pedestrian motion. *The Journal of Applied Mathematics and Physics (ZAMP)*, 64(2):223–251, June 2012.

[11] Hongkai Zhao. A fast sweeping method for eikonal equations. *Mathematics of Computation*, 74(250):603–627, May 2004.